SATELLITE-BASED PHENOLOGY ANALYSIS IN EVALUATING THE RESPONSE OF PUERTO RICO AND THE UNITED STATES VIRGIN ISLANDS' TROPICAL FORESTS TO THE 2017 HURRICANES

By

Melissa Collin

A Thesis Presented to

The Faculty of Humboldt State University

In Partial Fulfillment of the Requirements for the Degree

Master of Science in Natural Resources: Environmental Science & Management

Committee Membership

Dr. James Graham, Committee Chair

Dr. Kerry Byrne, Committee Member

Dr. Buddhika Madurapperuma, Committee Member

Dr. Erin Kelly, Program Graduate Coordinator

December 2021

ABSTRACT

SATELLITE-BASED PHENOLOGY ANALYSIS IN EVALUATING THE RESPONSE OF PUERTO RICO AND THE UNITED STATES VIRGIN ISLANDS' TROPICAL FORESTS TO THE 2017 HURRICANES

Melissa Collin

The functionality of tropical forest ecosystems and their productivity is highly related to the timing of phenological events. Understanding forest responses to major climate events is crucial for predicting the potential impacts of climate change. This research utilized Landsat satellite data and ground-based Forest Inventory and Analysis (FIA) plot data to investigate the dynamics of Puerto Rico and the U.S. Virgin Islands' (PRVI) tropical forests after two major hurricanes in 2017. Analyzing these two datasets allowed for validation of the remote sensing methodology with field data and for the investigation of whether this is an appropriate approach for estimating forest health in areas lacking *in-situ* data. I performed extensive cloud masking processes on the satellite imagery to produce masked, repaired, near cloud-free imagery, which were used to extract phenology metrics and produce annual phenology curves. FIA data was used to estimate forest percent mortality and change in aboveground live biomass (AGLB). Simple and multiple linear regression were used to explore the relationship between the FIA data and the remote sensing derived phenology metrics to analyze and compare trends. Phenology metrics showed a consistent trend of an initial decrease in index values the first year after the hurricanes, followed by a spike in values the second year after.

Consistent trends were seen after the hurricanes of a decrease in AGLB, an increase in mortality, and a decrease in phenology values the first year, followed by increase in values the second year after. Significant changes were found in AGLB and in the phenology metrics before and after the hurricanes, however there were no significant linear relationships found between the FIA data and the remote sensing data. Meaningful phenology curves were successfully generated when analyzing a small region with only one forest type and no data gaps. The results, therefore, help in constructing a base understanding of PRVI's tropical forests dynamic relative to climate change and give a clearer indication of the capabilities of the remotely sensed data. Furthermore, this research demonstrated approaches and techniques that can be further applied to larger, global sustainability goals to sustain living systems in times of climate variability and change.

ACKNOWLEDGEMENTS

This work was part of the Puerto Rico Sustainability Project, which was funded by the United States Forest Service, Grant number 19-CS-11120101-412. Research was in collaboration with Humboldt State University, Hong Kong Polytechnic University, the United States Forest Service – International Institute of Tropical Forestry, and the Southern Research Station.

Thank you to Sean Fleming, Dr. David Gwenzi, Dr. James Graham, Dr. Eileen Helmer, Dr. Xiaolin Zhu, Dr. Kerry Byrne, and Dr. Buddhika Madurapperuma for their guidance, advising, and expertise. Additionally, thank you to Mason Long, Humfredo Marcano, Dr. Yoon Kim, Kacie Flynn, and Angela Turner for their assistance. Lastly, thank you to my friends, family, and fellow graduate students for their support.

TABLE OF CONTENTS

LIST OF TABLES

LIST OF FIGURES

LIST OF APPENDICES

INTRODUCTION

Tropical forests occupy only about 8% of the Earth's land surface, yet they host the majority of our flora and fauna species (Gardner et al., 2009). These forests not only support endangered and rare species, but also provide valuable ecosystem services such as carbon sequestration and climate regulation (Asner et al., 2000; Miller & Lugo, 2009). While their importance is undisputed, it is unclear whether these forests can maintain their high levels of productivity in the face of anthropogenic climate change.

The functionality of tropical forest ecosystems and their productivity is highly related to the timing of phenological events (Lieberman, 1982). However, research on how these tropical forests respond to climate change and climatic events, such as drought and hurricanes, is limited. Understanding these responses to major climate events can help identify trends and patterns in forest resilience (Thompson et al., 2009; Isbell et al., 2015). This information is essential for forest management, biodiversity assessment, and ecosystem modeling.

Agricultural Abandonment

Most of Puerto Rico's forests today are not native old-growth, but are instead a mix of successional, naturalized vegetation, and young mixed-species stands. Within these secondary forests, many of the species are nonnatives that were introduced for ornamental, shade, fruit, or agroforestry, that became naturalized over time (Francis &

Liogier, 1991). These younger, secondary forests are a byproduct of industrialization and agriculture abandonment (Parés-Ramos et al., 2008).

By the 1940s in Puerto Rico, 90% of the forests had been cleared for various economical purposes, such as agriculture, charcoal production, and urban construction. It was at this time that the U.S. government and what is now the Puerto Rico Industrial Development Company implemented Operation Bootstrap, a series of projects to help transition the territory's economy from a rural agrarian to modern industrial (Rudel et al., 2000; Miller & Lugo, 2009).

As economic development occurred, there began a transition from agriculture to manufacturing. This movement of rural to urban migration resulted in vast agricultural abandonment (Rudel et al., 2000; Helmer et al., 2008; Parés-Ramos et al., 2008). Land that was previously greatly altered and shaped by land use practices was now suddenly left with little to no restoration. Over time forest succession occurred, transforming the abandoned pastures into secondary forests, where past disturbances are no longer evident on the landscape. Between 1940 to 2000, the island's forests increased from occupying approximately 6% of the island to 40%, occurring almost entirely on abandoned pastures and agricultural lands. However, these new forests did not return to their historic, native species, but instead are either mixed with or dominated by non-native, naturalized species (Parés-Ramos et al., 2008). These past events have provided an opportunity to research a unique and understudied tropical forest structure.

Phenology in Puerto Rico

Phenology is the study of cyclic and seasonal natural phenomena, specifically in relation to climate and plant and animal life. It can also be looked at as the seasonal timing of biological events and is crucial for long-term monitoring and trend analysis of biological systems. Climates with distinct seasonalities often have vegetation that has adapted to these phenological cycles (Kramer et al., 2000). If rapid climate change occurs within the life of a tree, it may be less adapted to the prevailing climate (Ostertag et al., 2005). Variation in phenology is a highly sensitive and influential factor in ecosystem function (Chen & Pan, 2002). Understanding short and long-term dynamics of phenology is key for evaluating the future of the ecosystems.

Puerto Rico's forests have distinct phenological cycles attributed to the region's uncommon seasonality, with not one, but two rainy seasons and two "dry" seasons (relative to Puerto Rico's tropical climate) each year (Gwenzi et al., 2017). This type of seasonality can be seen in many of the Caribbean islands. From April to June is the early rainy season, followed by a mild midsummer drought in July and August. August through November is the late rain season, where Puerto Rico reaches its peak greenness. This is succeeded by a long, dry winter from December to March, when peak brownness is reached.

The timing of the green up and brown down cycles can be detected by analyzing spatial and temporal variations. Vegetation indices, such as normalized difference vegetation index (NDVI) and enhanced vegetation index (EVI), can be applied to

imagery to measure plant greenness, indicating relative density and overall health of vegetation (Zhang, Friedl, & Schaaf, 2009; Wang et al., 2017a). Other indices such as normalized difference moisture index (NDMI) measure plant health by determine vegetation water content. Applying these indices to time series imagery allows for the detection of seasonal trends and the assessment of change in these patterns. These distinct seasonal patterns are a key component contributing to estimations such as aboveground live biomass (AGLB) which is a key sub-indicator of forest sustainability, as well as forest deciduousness, tree mortality, trait diversity, etc., and will be a base for future understanding of tropical forest dynamics in the face of climate change (Gwenzi et al., 2017).

Additionally, using these indices allows for the calculation of integral of the dry season. Integral of the dry season is a metric that is estimated using the start and end of the dry season and the integral of the spectral indices curve (Wei et al., 2012; Horion et al., 2014). Since the tropical forests of Puerto Rico and the U.S. Virgin Islands have unique seasonality, integral of the dry season may be a better measurement than the more common metric, length of the growing season, as it may better capture the changes that occur (E. Helmer, personal communication, May 21, 2021).

Hurricanes

Puerto Rico and the U.S. Virgin Islands are in the hurricane belt of the Caribbean and Western Atlantic, making them highly susceptible to frequent tropical cyclones. Tropical cyclones are rapidly rotating storm systems that produce squalls and heavy rain.

Hurricanes are a type of tropical cyclones that originate in the Atlantic and Northeastern Pacific, created in the summer and early fall as warm ocean water evaporates and twists into the atmosphere. The majority of these hurricanes form off the west coast of Africa between June and October and intensify as they travel across the warm Atlantic with the trade winds (Emanuel, 2003).

Most hurricanes that Puerto Rico encounters are peripheral and produce minor effects, however high intensity and direct hits can cause rapid, long-lasting damage to the island (Miller & Lugo, 2009). The level of damage caused to the tropical forests can range from leaf stripping and branch breaking to uprooting, stem damage, and ultimately tree mortality (Boose et al., 2004). This type of damage can alter regeneration and succession.

In September 2017, Puerto Rico was one of the many Caribbean islands devastated by two hurricanes, Hurricane Irma and Maria. Hurricane Irma formed off the north coast of Africa near the Cape Verde Islands in late August and intensified as it traveled across the Atlantic. When it reached Puerto Rico and the U.S. Virgin Islands on September 6th, it was a Category 5 hurricane, reaching maximum speeds of over 290 kilometers per hour (kph) (Cox et al., 2019). This hurricane was most devastating to the Virgin Islands, Culebra, Vieques, and Northeast Puerto Rico, a highly populated region and the location of the capital, San Juan. Nearly half the island lost power and over 80% of Puerto Rico's crops were destroyed.

About two weeks later, Puerto Rico and the Virgin Islands were struck again. Hurricane Maria formed east of the Lesser Antilles and hit Puerto Rico on September 20th

as a Category 4 (Cox et al., 2019). Unlike Irma, Maria's path crossed directly through the main island of Puerto Rico with winds up to 250 kph. Storm surges produced heavy rain, reaching up to 70 centimeters, causing widespread flooding around the island. The disaster greatly damaged the already weakened Puerto Rican power grid and left the entire territory without power (Tian & Zou, 2018). There were an estimated 3,000 causalities and billions of dollars in total damage. Possibly 40 million trees were killed or severely damaged, with the larger, older, and more established trees receiving the greatest damage (Gray, 2018). These older trees species, which are typically slower growing, provide important habitat to species that cannot reside in younger secondary forests (Tian & Zou, 2018).

Remote Sensing

Remote sensing is the process acquiring information and data remotely such as from a satellite or aircraft (Richards & Jia, 2006). Remote sensing can be very advantageous for research since so much of the data is open access, easily accessible, and is constantly being collected across the globe. A few examples of open access remotely sensed imagery are the National Aeronautics and Space Administration's (NASA) Landsat program, NASA's Moderate Resolution Imaging Spectroradiometer (MODIS), and the European Space Agency's Sentinel-2. This kind of data is especially important when researching remote, hard to reach regions and areas being affected by climatic events, as data can be collected rapidly and analyzed from a safe location. But there are also limitations to remote sensing, such as temporal and spectral resolution. Remote

sensing cannot replace the data and value that one can received from visiting a study site in person. Therefore, it is important, when possible, to have *in-situ* data, also referred to as on-the-ground data, to validate the results of the remotely sensed data. Having both types of datasets also allow us to assess the capabilities and further our understanding of remotely sensed data (Goetz et al., 1983). Ideally, if relationships and correlations can be found between the remotely sensed data and the on-the-ground data, analysis and estimates can be made without having to visit a site, as well as predict how future change will affect tropical forests (Gwenzi et al., 2017).

Literature Survey

Past research has analyzed the effects of hurricanes in tropical forests, with particular attention being paid to Hurricane Hugo, which hit Puerto Rico in 1989. These past studies focused on field surveying as their primary source of data collection. Field surveys allow for precise, detailed data collection; however, this approach can be very time consuming, expensive, and does not capture data across large landscapes. Researchers found no clear patterns in damage between species, but instead suggested size, spatial position, diameter growth rate, and past disturbance history as the strong variables in relation to resistance to damage (Ostertag et al., 2005). Strong winds from hurricanes remove substantial amounts of the canopy and break branches and stems. Tree mortality was found to be closely associated with stem breakage and uprooting, with fast-growing species being more susceptible to stem breakage. Where patterns were statistically detectable, the study found larger trees had higher mortality rates and

suffered greater overall damage after hurricanes than small trees (Lugo & Likens, 1992). Past studies also found that tree species commonly found in humid forests were least resistant to hurricane related damage (Brokaw & Grear, 1991; Zimmerman et al., 1994).

The use of remote sensing data is also commonly used by researchers to estimate plant health. Previous studies have used satellite imagery, drone imagery, and LiDAR to measure variables that are used to estimate forest biomass such as canopy height, area, and volume (Gwenzi et al., 2017). It is also used to estimate greenness, spatial pattern, and phenology factors (Wang et al., 2017b). This research provides a unique opportunity to harmonized field data with remote sensing, two methods of data collection with advantageous results.

Research Objectives

This study aimed to identify if tropical forest response to sudden disturbances, specifically hurricanes, can be detected with remote sensing. Using Puerto Rico and the U.S. Virgin Islands as a case study, this research focused on achieving two main objectives.

1. Quantify the effects of the 2017 hurricanes on tropical forest mortality and determine its relationship with Landsat derived phenology metrics.

2. Quantify the effects of the 2017 hurricanes on aboveground live biomass and determine its relationship with Landsat derived phenology metrics.

An additionally goal of the study was to generate meaningful phenology curves from the Landsat-derived phenology metrics to reflect the changes in trends across the island. Understanding these short and long-term dynamics of forest phenology will aid in

evaluating the future of these ecosystems. The results will be used to show phenology changes and aid in assessing forest vulnerability which could be used for forest management and restoration.

Rationale and Significance

As our climate continues to change, there will likely be more frequent and more extreme climatic events, such as hurricanes, and tropical regions will be greatly affected (Mann & Emanuel, 2006). Tropical forests occupy only a small portion of Earth; however, they are home to the majority of our species, and play a critical role in ecosystem services (Gardner et al., 2009). Puerto Rico and the U.S. Virgin Islands' extreme climatic events paired with an abundance of available data (Landsat and Forest Inventory and Analysis data) offers a unique research opportunity. Better understanding climatic events such as hurricanes gives insight into the challenges they create and aid in mitigating their effects. This research also helps in resolving uncertainties in modeling tropical forest dynamics and improving precision in future forest ecosystem modeling (Hilibrand & Robbins, 2004).

Results from this study allows researchers to better identify the forests most susceptible and resilient to hurricane-related events. This gives forest managers a stronger understanding of forest vulnerability. This helps with the promotion and implementation of sustainable management of all types of forests, and informs people and groups involved in forest conservation, as well as those involved in harvesting and reforesting. Lastly, this research demonstrates approaches and techniques used on Puerto Rico and

the U.S. Virgin Islands that can further be applicable to larger, global sustainability goals, such as the NASA supported Sustainable Development Goal 15, to halt biodiversity loss and sustain living systems in a time of climate variability and change (Hilibrand & Robbins, 2004).

METHODS

Due to the confidentiality of plot locations, some analysis and data extraction was conducted by the Principal Investigator (PI), Dr. David Gwenzi, a professor and my former graduate advisor from Humboldt State University, and the co-PI, Dr. Eileen Helmer, a research ecologist from the USFS – International Institute of Tropical Forestry. Additionally, many of the IDL and R scripts used in this study were written by a project collaborator, Dr. Xiaolin Zhu, a professor at Hong Kong Polytechnic University. Work conducted by the PI and co-PI is specified in the relevant sections. All other analysis was conducted by myself unless stated otherwise.

Data Collection

Study Site

The region of interest for this study was Puerto Rico and the U.S. Virgin Islands (PRVI). Puerto Rico and the U.S. Virgin Islands are unincorporated United States territories located in the North Caribbean Sea, approximately 1,850 kilometers southeast of Florida (Figure 1). The main island of Puerto Rico has an area of approximately 8,900 km^2. Puerto Rico is part of the Greater Antilles, the island group consisting of Puerto Rico, Cuba, Hispaniola (Haiti and the Dominican Republic), Jamaica, and the Cayman Islands. In total, the Greater and Lesser Antilles are approximately 7,000 islands and are part of the West Indies. Puerto Rico consists of the main island of Puerto Rico and five smaller islands, Vieques, Culebra, Mona, Desecheo, and Caja de Muertos. Of the five

smaller islands, Culebra and Vieques are the only ones inhabited year-round (Miller & Lugo, 2009).

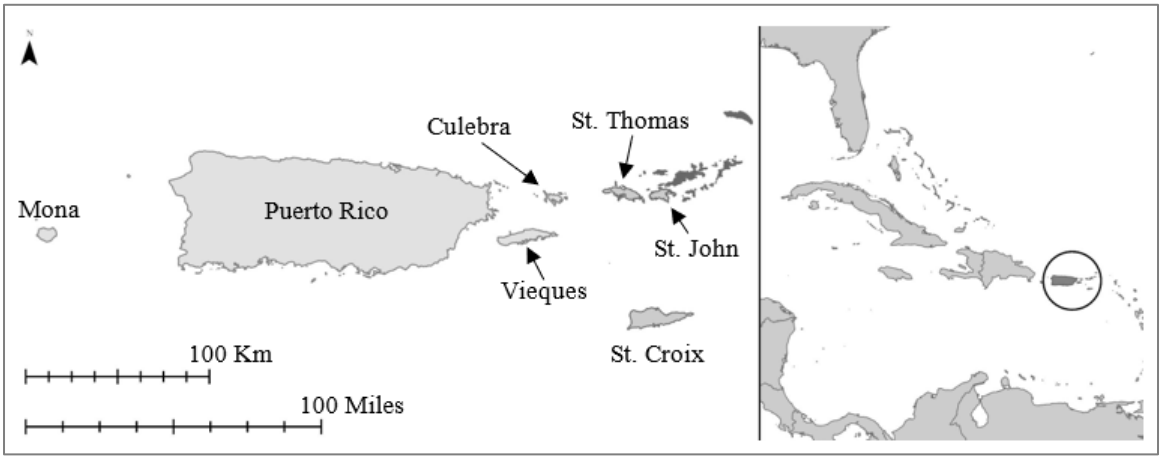

Figure 1: Puerto Rico and the U.S. Virgin Islands. Data Sources: Natural Earth, OCHA, U.S. Census Bureau.

Puerto Rico is located in the tropics, giving it a maritime climate with warm temperatures with minimal fluctuation. Rainfall varies greatly across the island because of its dynamic topography. Average annual precipitation ranges from 745mm in Magueyes Island to 4,346 mm in Pico del Este. The island can be broken into three major physiographic regions: high mountains, foothills, and coastal plains. Nearly all the coastal plains have been converted for either agriculture, roads, or urban. Puerto Rico can also be broken up by ecological life zones based on factors such as latitude, elevation, temperature, and precipitation. While this study only separated forest types by either dry or humid forests, Puerto Rico can be divided further into six major life zones: subtropical dry forest, subtropical moist forest, subtropical rainforest, subtropical wet forest, lower montane rain

forest, and lower montane wet forest (Ewel & Whitmore, 1973). The subtropical moist forest is overwhelmingly the largest of the life zones, however most of it was deforested for agriculture before 1930 (Miller & Lugo, 2009). Analysis was conducted on the main island of Puerto Rico, the smaller islands Mona, Culebra, and Vieques, and the three main U.S. Virgin Islands of Saint Croix, Saint John, and Saint Thomas.

Time Frame and Data Selection

This research was split into four time frames: January 1, 2010 to December 31, 2014 (2010-2014), September 1, 2016 to September 1, 2017 (2016-2017), October 1, 2017 to October 1, 2018 (2017-2018), and November 1, 2018 to November 1, 2019 (2018-2019). The first time frame, January 2010 to December 2014, established consistent, pre-hurricane conditions. 2010-2014 were four consecutive years with no major climatic events, such as hurricanes or drought, which also corresponded with the FIA inventory cycle for PRVI. 2015 and the first half of 2016 were excluded from the study due to the drought that occurred across PRVI during that time. The second time frame, September 2016 to September 2017, was one full year leading up to the hurricanes, which occurred on September 6th and September 20th of 2017. The third and fourth time frames, October 2017 to October 2018 and November 2018 to November 2019, captured the two years directly after the hurricanes.

The satellite imagery used in the study were surface reflectance products from Landsat 8 OLI/TIRS C1 Level-2, Landsat 7 ETM+ C11 Level-2, and Landsat 5 TM C1 Level-2. Landsat is the longest running continuous satellite program, run by NASA and

the United States Geological Survey (USGS). Landsat imagery has numerous spectral bands with, a 30 by 30-meter spatial resolution (900 m^2), and a 16 day revisit time (Williams et al., 2006). All satellite imagery was downloaded from the USGS Earth Explorer website (https://earthexplorer.usgs.gov/). Five Landsat scenes were needed to capture all of Puerto Rico and the U.S. Virgin Islands (Table 1).

Table 1: The path, row, scene generalized name of the Landsat imagery used.

Path	Row	Scene generalized name
6	47	Mona
5	47	Main (Northwest and Central Puerto Rico)
4	47	North East (Northeast Puerto Rico, Vieques, Culebra, St Thomas, and St John)
5	48	South West (Southwest Puerto Rico)
4	48	South East (Southeast Puerto Rico and St Croix)

When selecting imagery from these datasets, only images estimated to contain less than 50% land cloud coverage were downloaded. Imagery with large amounts of cloud cover greatly limits its use in analysis. Additionally, the cloud masking algorithm performance decreases on images with greater than 50% cloud cover.

Field data used in this study was from the FIA program. FIA data was collected by the United States Forest Service (USFS) and plot-level summaries across Puerto Rico and the U.S. Virgin Islands were prepared by the co-PI. Each plot is approximately 36 x 36 meters (1,296 m^2), is representative of roughly 6,000 acres, and is selected semi-randomly using a hexagonal grid (USDA, 2014). FIA data was utilized from the inventory cycles between 2011-2014 and 2016-2019, which were separated into the four time frames. Inventories occurred in different locations across the study site depending on the year surveyed (Table 2, Appendix A and B). The PI extracted data and provided

the plot numbers and associated metrics which allowed me to join the FIA data with the remote sensing data without revealing confidential plot locations.

Table 2: Number of FIA plots sampled for aboveground live biomass in each region for each time frame. There's a combined total of 379 plots, 278 of which were sampled on the main island of Puerto Rico.

Region (abbrev.)	2010-14	2016-17	2017-18	2018-19	Total
Northwest and Central Puerto Rico (Main)	105	66	28		199
Northeast Puerto Rico (NEMain)	13	11	3		27
Southeast Puerto Rico (SEMain)	6	5	1		12
Southwest Puerto Rico (SW)	21	14	5		40
Mona (Mona)	25				25
Vieques (NE1)	16			16	32
Culebra (NE2)	8			7	15
St Croix (SE1)	14				14
St Thomas and St John (NE3)	15				15
Total	223	96	37	23	379

After the satellite data and FIA data was selected and acquired, I began analysis. The methodology was conducted in three segments: image preprocessing, image analysis, and statistical analysis (Figure 2).

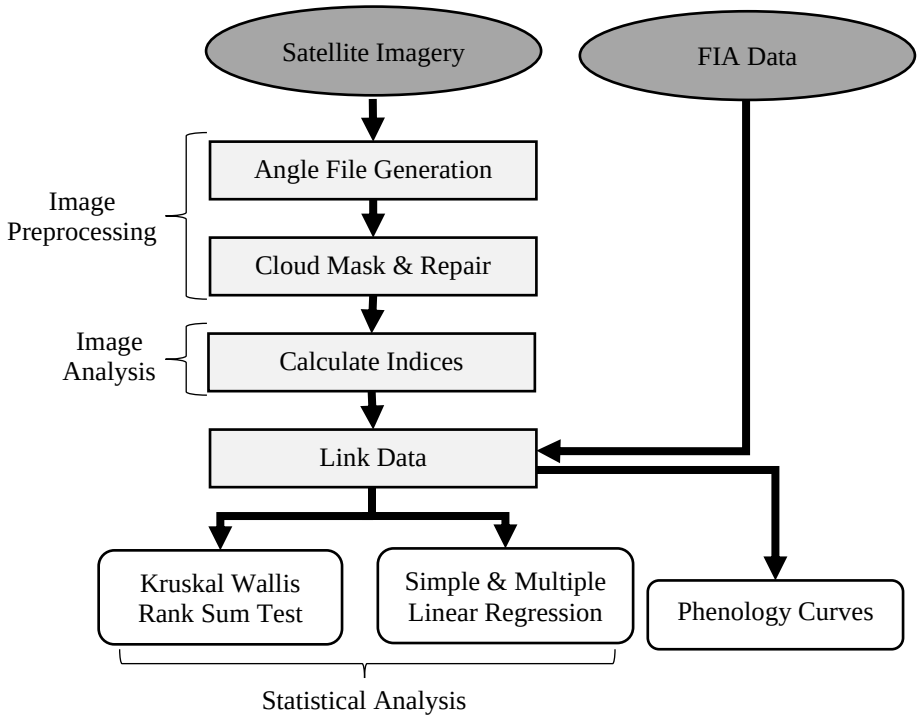

Figure 2: A flow chart outlining the methodology for processing, merging, and analyzing the satellite imagery and the FIA plot data.

Image Preprocessing

Intensive preprocessing was conducted on the downloaded satellite imagery prior to data analysis. I downloaded imagery from September 1, 2016 to September 1, 2017, October 1, 2017 to October 1, 2018, and November 1, 2018 to November 1, 2019. Repaired Landsat imagery from January 1, 2010 to December 31, 2014 was provided by the PI who conducted the downloading and image preprocessing for that time frame.

Angle File Generation

First, I made solar and sensor angle bands using the USGS's Landsat Angle Creation Tool. These bands provide per-pixel solar and sensor azimuth and zenith values, which are necessary for the cloud masking process. I used Oracle VM Virtual Box to create an Ubuntu Linux virtual machine, since the tool can only be used in a Linux environment. I downloaded angle coefficient files off the USGS EarthExplorer website and extracted them from the Level 1 top of atmosphere (TOA) products for the corresponding Level 2 surface reflectance (SR) images. I then brought these angle coefficient files into the virtual machine and input them into the Angle Creation Tool. I wrote and executed a python script to automate the file generation. I then moved the generated solar and sensor files out of the virtual machine, renamed to match Landsat's nomenclature, and converted to Tagged Image File Format (TIFF) files using R.

Cloud Masking and Repairing Time Series Images

Next, I executed a series of steps to create the time series, mask for clouds, and repair the final time series images, using the remote sensing software Environment for Visualizing Images (ENVI) and the programming language Interactive Data Language (IDL). I conducted these processes for each time frame using R codes and a set of IDL codes created by Dr. Zhu and Dr. Gwenzi (Helmer et al., 2018; Zhu & Helmer, 2018). The following paragraph outlines the processes I ran using these codes.

After the Landsat satellite imagery was obtained from the EarthExplorer website, I used a bidirectional reflectance distribution function (BDRF) to normalize pixel values across the scenes with codes from Roy et al., 2016. BDRF accounts for different effects

caused by the angle of the satellite and the angle of the sun when the image was taken, or view zenith and solar zenith respectively. BRDF combats this by adjusting the view zenith to 0° and the solar zenith to 30° for each scene. Next, I reordered the images based on the day of the year the image was taken (*i.e.*, February 5 = 36, December 31 = 365), regardless of the actual year, and then stacked them together into a time series. This prepared the images for the masking process. Using ENVI, I used a water mask corresponding with the region to indicate what pixels in the image represent water and what pixels represent land. Water was not within my scope of interest, and therefore was masked out from any further steps to reduce the processing time. I then used the Automatic Time-Series Analysis (ATSA) algorithm to screen clouds and cloud shadows in the imagery (Zhu & Helmer, 2018). This multistep method works by first calculating clouds/cloud shadow indices and generating initial cloud and shadow masks. The masks are then refined using the time series image stack to identify, omit, and interpolate the masked images. The nearest similar pixel interpolator (NSPI) algorithm was then used to estimate and fill any missing data values and produces the final repaired time series images (Zhu et al., 2012, Zhu et al., 2019).

Image Analysis

Spectral Indices

I used the repaired Landsat images to compute spectral indices, which are combinations of spectral reflectance values from multiple spectral bands that indicate abundance of a feature of interest (Jackson, 1983). Each index provides varying

adjustments and sensitivities to better detect different aspects of vegetation. The three spectral indices I utilized in this study were enhanced vegetation index (EVI), normalized difference vegetation index (NDVI), and normalized difference moisture index (NDMI) (Wang et al., 2017). The Enhanced Vegetation Index measures vegetation greenness, specifically canopy type and leaf area index, while also correcting for atmospheric conditions and noise. The EVI equation is as follows:

$$EVI = G * \frac{(NIR - Red)}{(NIR + C1 * Red - C2 * Blue + L)}$$

Where NIR/Red/Blue are atmospherically corrected surface reflectance values, L is the canopy correction factor (1.0), C1 and C2 are coefficients for atmospheric resistance (6.0 and 7.5 respectively), and G is gain factor (2.5). Next, the Normalized Difference Vegetation Index also detects greenness by measuring vegetation health and vigor. The NDVI equation is as follows:

$$NDVI = \frac{NIR - Red}{NIR + Red}$$

Where the Near Infrared Band (NIR) and the Red Band (Red) are atmospherically corrected surface reflectance values. Last, the Normalized Difference Moisture Index measures vegetation water content/water stress. The NDMI equation is as follows:

$$NDMI = \frac{NIR - SWIR}{NIR + SWIR}$$

Where NIR and the Short-wave Infrared Band (SWIR) are atmospherically corrected surface reflectance values. I extracted the spectral indices using a series of IDL codes written by Dr. Zhu. Final spectral index images were sent to the co-PI., who conducted the following steps to extract and summarize plot level phenology metrics. To extract

metrics, the co-PI assigned FIA plots a phenology value by averaging the values of the plot's surrounding Landsat pixels. Some phenology metrics were transformed before averaging pixel values in a window. Each index value was extracted and averaged from a 3x3 pixel window corresponding with each FIA plot locations. This produced an accurate plot level approximation since a 3x3 Landsat pixel window is roughly the same size as an FIA plot. Once the phenology metrics were extracted and calculated, the co-PI sent the data back to me for further statistics.

Phenology Curves

I generated phenology curves using the phenology metrics that the PI created and extracted from the repaired time series images. Extracted values from across the study site were combined and averaged to create a mean value for each time window. I plotted values on a line graph with the index values on the y-axis and the day of the year on the x-axis to created phenology curves. I made additional curves using only values from plots on the island of Mona.

Linking the Data

I combined plot level phenology metrics extracted from satellite imagery and FIA data into a single dataset in Microsoft Excel using the plot numbers as the common link. Merging these two datasets allowed me to relate field data with remotely sensed data.

Statistical Analysis

I conducted all analysis involving FIA data (AGLB and mortality) at the plot level to investigate for relationships between the data and anomalies in phenology. Analyses were conducted on all fully forested plots, on all fully forested plots separated into two habitat types: dry forests (subtropical dry forest) and humid forests (subtropical moist forest, subtropical rain forest, lower montane rain forest, lower montane wet forest, and subtropical wet forests), and on fully forested plots only on the main island of Puerto Rico. I generated boxplots and histograms for both AGLB and mortality to visually assess distributions, patterns, and trends in the data. Data transformations such as logarithmic and square root were tested, but ultimately not kept as they failed to successfully fit the data to a more normal distribution.

For analyzing aboveground live biomass, the two variables I utilized were 1. total aboveground live biomass (saplings + trees) in megagrams of dry mass per hectare (Mg/ha) and 2. net growth in aboveground live biomass in Megagrams of dry mass per hectare of forest per year (Mg/ha/yr), which herein is referred to as AGLB and AGLB net change, respectively. These variables were generated by the co-PI using models from the FIA program. For AGLB, tree-level aboveground live biomass was estimated using diameter at breast height and tree height to estimate main stem volume, and allometric ratios were used to estimate biomass of tree components (Burrill et al., 2018). Per hectare biomass was derived by summing values of saplings and trees from the subplots and microplots, then dividing by the forested area of the plot. For AGLB net change, net

biomass growth/loss was calculated by summing the growth of survivors from the previous inventory cycle (t1) and the new growth from the current inventory cycle (t2), then subtracting the mortality from the previous inventory cycle (t1).

For analyzing mortality, each plot had survival and mortality data, which showed the number of individuals that died and the number of individuals that survived. Individual plants/vegetation was separated into three categories: saplings, small trees, and large trees. Saplings were classified as saplings or seedlings of any size, small trees were classified as trees with less than 5 inches diameter breast height (d.b.h.), and large trees were classified as trees with greater than or equal to 5 inches d.b.h. Using these variables, I calculated percent mortality for saplings, small trees, large trees with the following formula:

$$\frac{Mortality\ Count}{Surival\ Count + Mortality\ Count}$$

Where mortality count is the number of individuals in the plot that died, and survival count is the number of living individuals in the plot.

Kruskal-Wallis Rank Sum Test

I conducted the Kruskal-Wallis Rank Sum test on the following variables to test for significant differences among the four-time frames: AGLB, AGLB net change, and the maximum (max) value, minimum (min) value, and integral of the dry season for each of the indexes, EVI, NDMI, and NDVI. Kruskal-Wallis was chosen as an alternative, non-parametric method to ANOVA because the data did not meet the assumptions

required for ANOVA (normal distributions and homogeneity of variances) (Hecke, 2012). The Kruskal-Wallis Rank Sum Test equation is as follows:

$$K = \left[\frac{12}{N(N+1)}\sum\frac{T_i^2}{n_i}\right] - 3(N+1)$$

Where *N* is the sum of all sample sizes, T^i is the sum of ranks for the $_i$th sample, and n_i is the size of the $_i$th sample.

Dunn's Test of Multiple Comparisons

I conducted the Dunn's Test of Multiple Comparisons, a nonparametric pairwise test which follows up a significant Kruskal-Wallis test to determine which group or groups are statistically different from one another (Dinno, 2015). This test was conducted on each variable listed above for the Kruskal-Wallis test that received a significant test result. The Dunn's Test of Multiple Comparisons formula to calculate the z-test statistic for the difference between two groups is as follows:

$$z_i = \frac{y_i}{\sigma_i}$$

Where i is one of the 1 to m multiple comparisons, $y_i = W_A - W_B$ (Where W_A is the average of the sum of the ranks for it ith group) and σ_i is calculated as:

$$\sigma_i = \sqrt{\left\{\frac{N(N+1)}{12} - \frac{\sum_{s=1}^{T} T_s^3 - T_s}{12(N-1)}\right\}\left(\frac{1}{n_A} + \frac{1}{n_B}\right)}$$

Where N is the total number of observations across all groups, r is the number of tied ranks, and T_s is the number of observations tied at the specific tied value.

Simple and Multiple Linear Regression

I used simple and multiple linear regression to assess the degree to which the FIA data (AGLB, mortality) were linearly related to the satellite data (EVI, NDVI, NDMI). For analysis on biomass change, multiple linear regression was conducted using AGLB and AGLB net change as response variables and max index values, min index values, and integral of the dry season for each spectral index as predictor variables. The formula for multiple linear regression is as follows:

$$Y' = b_0 + b_1X_1 + b_2X_2 + \ ... + b_pX_p$$

Where Y' is the predicted value of the dependent variable, X_1 through X_p are predictor variables, b_0 is the values of Y when the independent variables are equal to zero, and b_1 through b_p are the estimated regression coefficient (LaMorte, 2016).

For mortality analysis, I conducted multiple linear regression using percent mortality of saplings, percent mortality of small trees, and percent mortality of large trees as response variables and max index values, min index values, and integral of the dry season for each spectral index as predictor variables.

Additionally, I conducted simple linear regression on percent mortality and delta maximum index, or Δ_{max} index. Δ_{max} index was calculated by linking plots using the previous plot number, then subtracting the max index values of the current inventory cycle (t2) from the max index values from the previous inventory cycle (t1). The formula for simple linear regression is as follows:

$$Y' = b_0 + b_1X_1$$

Where $\hat{Y}$ is the predicted value of the dependent variable, X_1 is the predictor variable, b_0 is the values of Y when the independent variable is equal to zero, and b_1 is the estimated regression coefficient (LaMorte, 2016).

RESULTS

Phenology Metrics

The three spectral indices (EVI, NDMI, and NDVI) were visualized using boxplots to analyze the spread of the datasets and the change across the time frames. In each figure showing box and whisker plots, X's indicate the mean value, the lower boxes show the 1st quantile, the top boxes show the 3rd quantile, both separated in the middle by the median line. The whiskers showing the min and max values for each time frame and for each graph outliers were removed. Box and whisker plots were chosen for visualization because the data was not normally distributed. During the post-hurricane period, there was an initial drop in index values of humid forests directly after the 2017-2018 time frame. However, in the following year, 2018-2019, there was a spike in humid forest values, exceeding the two pre-hurricane time frames (Figures 3, 4, and 5). Dry forests were less effected, i.e. maintained similar index values across time frames and only showing small changes in the distribution of values.

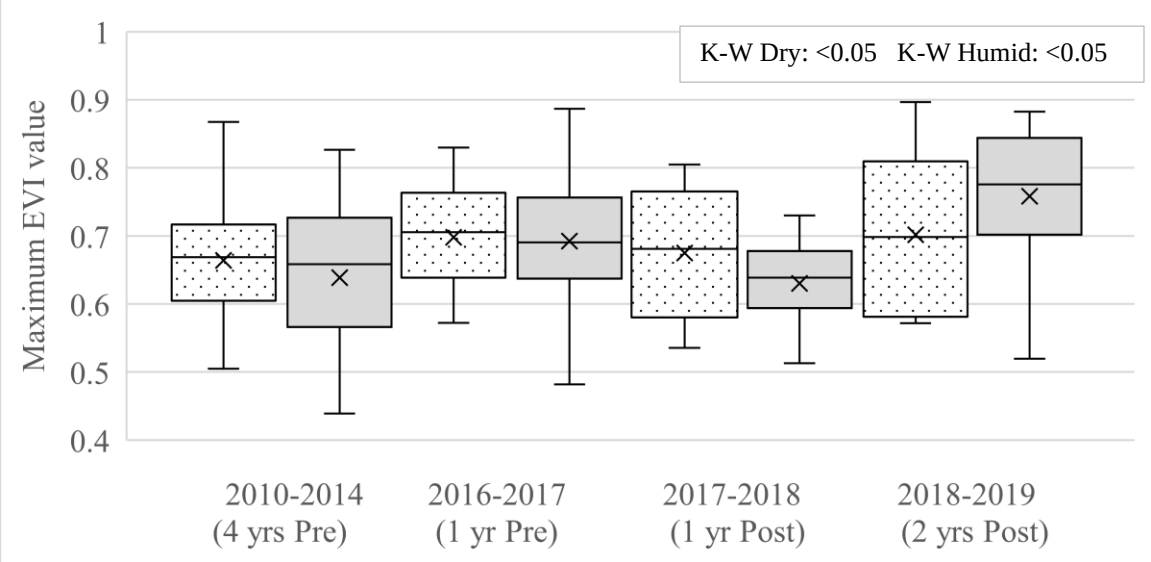

Figure 3: Plot level maxEVI values separated by dry forests (white boxes with black dots) and humid forest (grey boxes) for each time frames. K-W are the p-value results for the Kruskal-Wallis test.

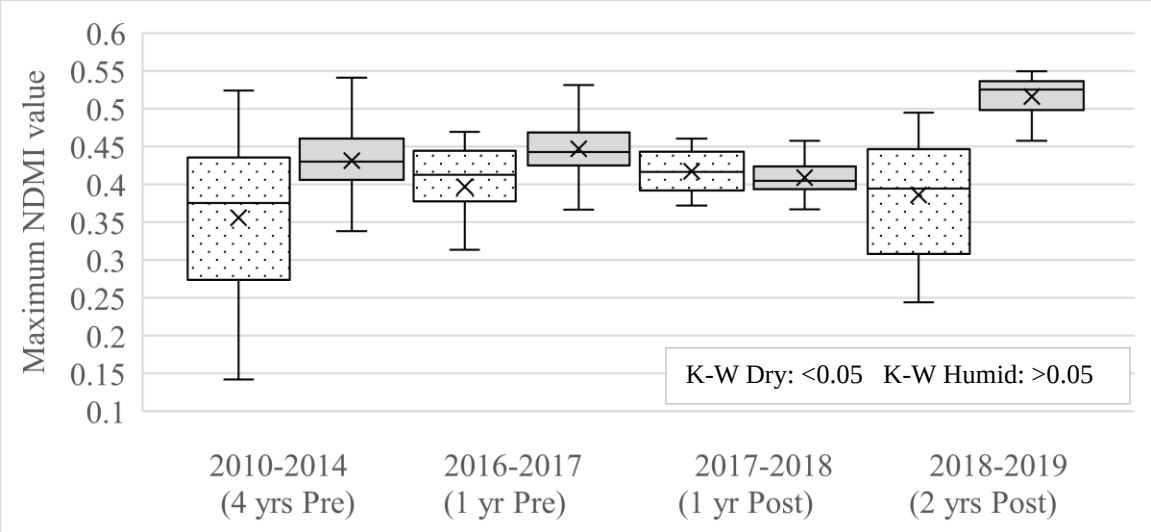

Figure 4: Plot level maxNDMI values separated by dry forests (white boxes with black dots) and humid forest (grey boxes) for each time frames. K-W are the p-value results for the Kruskal-Wallis test.

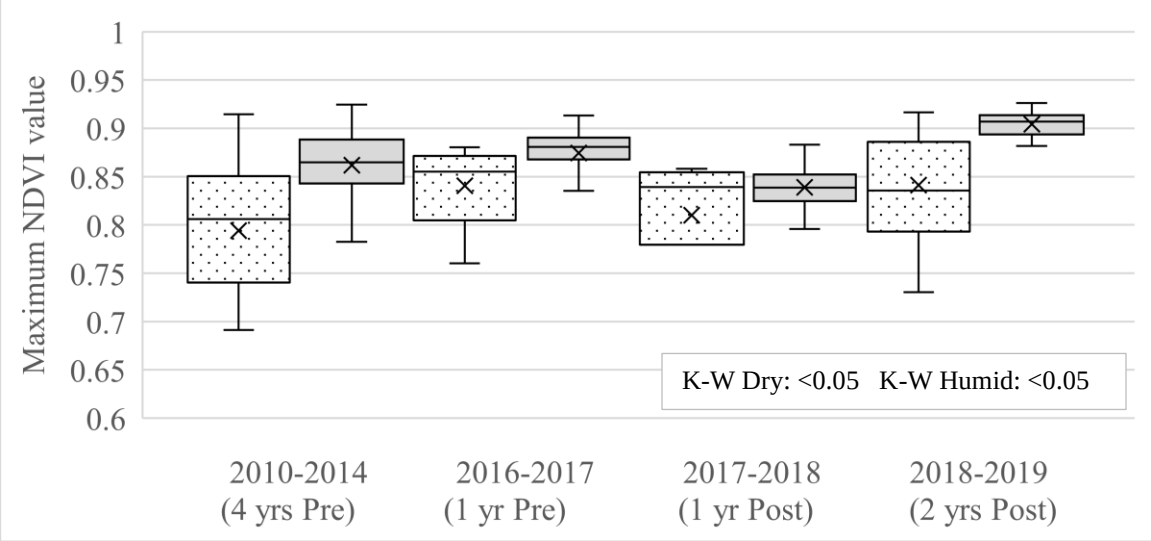

Figure 5: Plot level maxNDVI values separated by dry forests (white boxes with black dots) and humid forest (grey boxes) for each time frames. K-W are the p-value results for the Kruskal-Wallis test.

Every Kruskal-Wallis Rank Sum Test conducted on the spectral indices, with the exception of maxNDMI values for dry forest, showed significant differences ($p < 0.05$) among the time frames. Results for the Dunn's Test of Multiple Comparisons conducted on the spectral indices showed that almost every time frame, regardless or whether it was a pre-hurricane or post-hurricane time frame, was significantly different from each other (Table 3). When conducted on dry and humid forests separately, I saw more significant differences when comparing time frames in the humid forest (Appendix C and D).

Table 3: Results of Dunn's Test on phenology metrics for **all forests** in **PRVI**. Comparison columns indicates the two time frames being compared (1 = 2010-2014, 2 = 2016-2017, 3 = 2017-2018, 4 = 2018-2019). Pre-hurricane time frames are in orange and post-hurricane time frames are in blue. An adjusted p-value (P. adj) of <0.05 indicates the two time frames being compared are significantly different from each other.

Index Type	Comparison 1 (EVI)	Comparison 2 (EVI)	P. adj (EVI)	Comparison 1 (NDMI)	Comparison 2 (NDMI)	P. adj (NDMI)	Comparison 1 (NDVI)	Comparison 2 (NDVI)	P. adj (NDVI)
Max	1	2	<0.05	1	2	<0.05	1	2	<0.05
Max	1	3	1.00	1	3	0.71	1	3	<0.05
Max	2	3	<0.05	2	3	<0.05	2	3	<0.05
Max	1	4	<0.05	1	4	<0.05	1	4	<0.05
Max	2	4	0.87	2	4	1.00	2	4	1.00
Max	3	4	<0.05	3	4	<0.05	3	4	<0.05
Min	1	2	<0.05	1	2	<0.05	1	2	<0.05
Min	1	3	<0.05	1	3	1.00	1	3	1.00
Min	2	3	<0.05	2	3	<0.05	2	3	<0.05
Min	1	4	<0.05	1	4	<0.05	1	4	<0.05
Min	2	4	<0.05	2	4	<0.05	2	4	<0.05
Min	3	4	<0.05	3	4	<0.05	3	4	<0.05
IntDry	1	2	0.12	1	2	<0.05	1	2	<0.05
IntDry	1	3	1.00	1	3	1.00	1	3	1.00
IntDry	2	3	0.22	2	3	<0.05	2	3	<0.05
IntDry	1	4	<0.05	1	4	<0.05	1	4	<0.05
IntDry	2	4	0.23	2	4	1.00	2	4	1.00
IntDry	3	4	<0.05	3	4	<0.05	3	4	<0.05

Aboveground Live Biomass

The FIA data (AGLB, mortality) exhibited slightly different, but more expected trends than the spectral indices across the time frames. Directly after the hurricanes in 2017-2018, AGLB had an increase in range for dry forests, while humid forest remained relatively unchanged (Figure 6). These values and ranges dropped drastically 2 years after the hurricane in the 2018-2019 time period. AGLB net change (Figure 7) on the other hand dropped/decreased in the first post-hurricane time frame (2017-2018), and unlike the spectral indices, showed little to no recovery in the second post-hurricane time frame (2018-2019). Unlike the spectral indices, AGLB showed variability in both dry and humid forests.

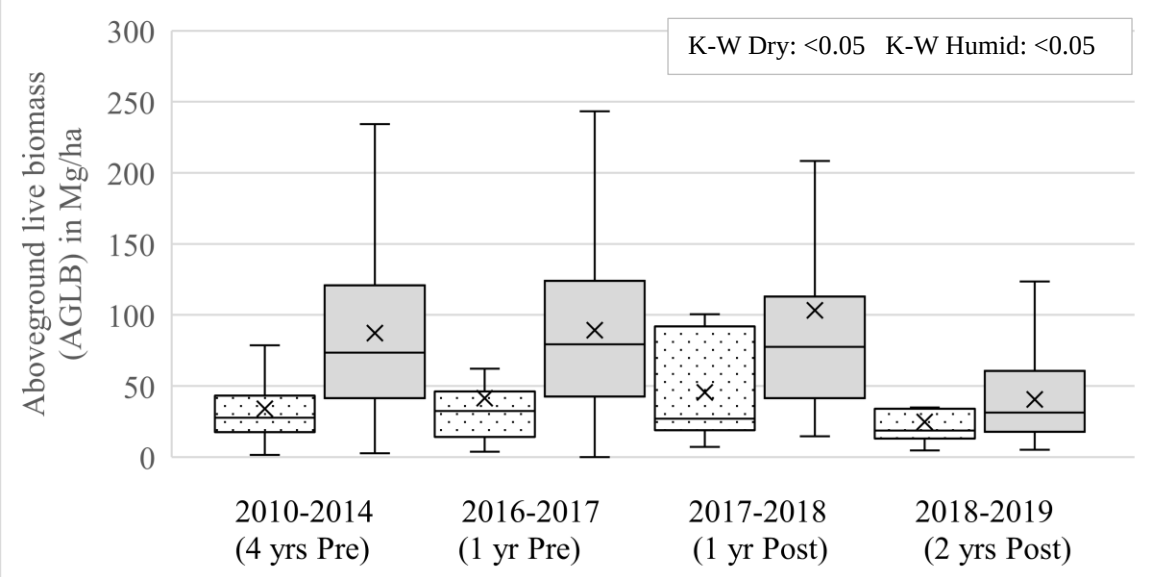

Figure 6: Plot level AGLB values separated by dry forests (white boxes with black dots) and humid forest (grey boxes) for each time frames. K-W are the p-value results for the Kruskal-Wallis test.

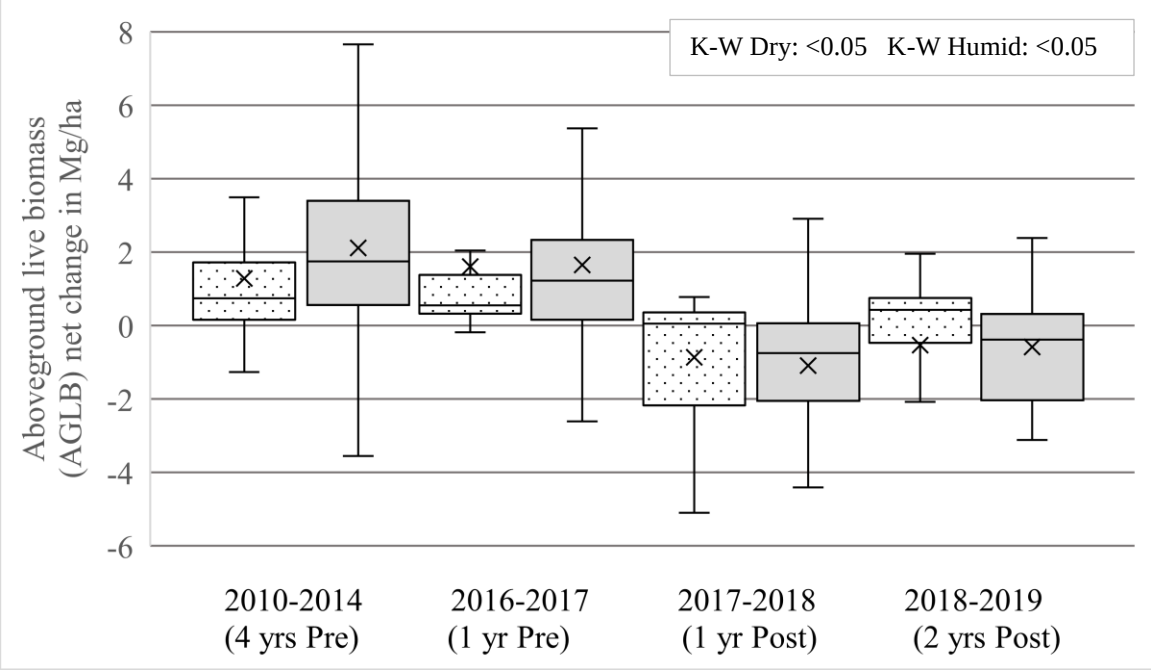

Figure 7: Plot showing plot level AGLB net change values separated by dry forests (white boxes with black dots) and humid forest (grey boxes) for each time frames. K-W are the p-value results for the Kruskal-Wallis test.

The Kruskal-Wallis Rank Sum Test on AGLB for all forests (both dry and humid forests combined) showed an overall significant difference (p-value=0.0001) among the 4 time frames. However, when separated by habitat type, only humid forests showed significant differences (p=0.02), while dry forests showed no significant differences (p=0.55). AGLB net change was significantly different (p=7.10e-11) among the 4-frames for both dry and humid forests combined as well as when separated by habitat types (p=0.01 for humid forests and p=0.02 for dry forests).

Results from the Dunn's Test of Multiple Comparisons conducted on AGLB showed that only the 2018-2019 time frame was significantly different from the other 3 time frames (Table 4). 2010-2014, 2016-2017, and 2017-2018 were not significantly

different when compared to each other. Results from the Dunn's test on AGLB net change showed that the two pre-hurricane time periods (2010-2014 and 2016-2017) were not significantly different from each other and the two post-hurricane time periods (2017-2018 and 2018-2019) were not significantly different from each other (Table 5). However, when comparing a pre-hurricane time period and a post-hurricane time periods (2010-2014 and 2017-2018, 2010-2014 and 2018-2019, 2016-2017 and 2017-2018, or 2016-2017 and 2018-2019) there were significant differences between the two time frames.

Table 4: Results of Dunn's Test on **AGLB** for **PRVI**. Comparison columns indicates the two time frames being compared (1 = 2010-2014, 2 = 2016-2017, 3 = 2017-2018, 4 = 2018-2019). Pre-hurricane time frames are in orange and post-hurricane time frames are in blue. An adjusted p-value (P. adj) of <0.05 indicates the two time frames being compared are significantly different from each other.

Comparison 1 (ALL)	Comparison 2 (ALL)	P. adj (ALL)	Comparison 1 (DRY)	Comparison 2 (DRY)	P. adj (DRY)	Comparison 1 (HUMID)	Comparison 2 (HUMID)	P. adj (HUMID)
1	2	0.17	1	2	1.00	1	2	1.00
1	3	0.41	1	3	1.00	1	3	1.00
2	3	1.00	2	3	1.00	2	3	1.00
1	4	<0.05	1	4	1.00	1	4	<0.05
2	4	<0.05	2	4	1.00	2	4	<0.05
3	4	<0.05	3	4	1.00	3	4	<0.05

Table 5: Results of Dunn's Test on **AGLB net change** for **PRVI**. Comparison columns indicates the two time frames being compared (1 = 2010-2014, 2 = 2016-2017, 3 = 2017-2018, 4 = 2018-2019). Pre-hurricane time frames are in orange and post-hurricane time frames are in blue. An adjusted p-value (P. adj) of <0.05 indicates the two time frames being compared are significantly different from each other.

Comparison 1 (ALL)	Comparison 2 (ALL)	P. adj (ALL)	Comparison 1 (DRY)	Comparison 2 (DRY)	P. adj (DRY)	Comparison 1 (HUMID)	Comparison 2 (HUMID)	P. adj (HUMID)
1	2	1.00	1	2	1.00	1	2	<0.05
1	3	<0.05	1	3	0.07	1	3	<0.05
2	3	<0.05	2	3	0.16	2	3	<0.05
1	4	<0.05	1	4	0.22	1	4	<0.05
2	4	<0.05	2	4	0.56	2	4	<0.05
3	4	1.00	3	4	1.00	3	4	1.00

Multiple linear regression was conducted on PRVI to analyze the relationship between AGLB and max index, min index, and integral of the dry season (Table 6). For regression with AGLB, significant p-values were found for max and min values for the indices, almost exclusively in the pre-hurricane time frames (2010-2014 and 2016-2017). Integral of the dry season yielded no significant results for any indices. For regression with AGLB net change, NDMI yielded p-values of less than 0.05 for all three spectral indices in the 2018-2019 window (Table 7). When the multiple linear regression was run on dry and humid forests separately, only significant p-values were found in humid forests (Table 8, 9, 10, and 11). However, for all regression analysis that produced significant p-values, none produced any high adjusted R-squared values, ranging from only 0.07 to 0.27.

Table 6: P-values from multiple linear regression, conducted on **all forests** of **PRVI** for **AGLB** and max index, min index, and integral of the dry season for EVI, NDMI, and NDVI.

Index	Index Type	2010-2014	2016-2017	2017-2018	2018-2019
EVI	Max	0.97	**< 0.05**	0.39	0.61
EVI	Min	**< 0.05**	0.61	0.65	0.43
EVI	IntDry	0.73	0.23	0.68	0.28
NDMI	Max	0.95	0.23	**< 0.05**	0.98
NDMI	Min	**< 0.05**	**< 0.05**	0.11	0.82
NDMI	IntDry	0.52	0.12	0.06	0.19
NDVI	Max	**< 0.05**	**< 0.05**	0.08	0.95
NDVI	Min	0.09	0.42	0.15	0.44
NDVI	IntDry	0.18	0.33	0.06	0.9

Table 7: P-values from multiple linear regression, conducted on **all forests** of **PRVI** for **AGLB net change** and max index, min index, and integral of the dry season for EVI, NDMI, and NDVI.

Index	Index Type	2010-2014	2016-2017	2017-2018	2018-2019
EVI	Max	0.45	0.64	0.83	0.23
EVI	Min	0.67	0.94	0.66	0.19
EVI	IntDry	0.94	0.35	0.55	0.52
NDMI	Max	0.67	0.4	0.84	**< 0.05**
NDMI	Min	0.53	0.14	0.68	**< 0.05**
NDMI	IntDry	0.8	0.38	0.62	**< 0.05**
NDVI	Max	0.43	0.89	0.46	0.06
NDVI	Min	0.64	0.89	0.51	**< 0.05**
NDVI	IntDry	0.62	0.39	0.5	0.69

Table 8: P-values from multiple linear regression, conducted on only **dry forests** of **PRVI** for **AGLB** and max index, min index, and integral of the dry season for EVI, NDMI, and NDVI.

Index	Index Type	2010-2014	2016-2017	2017-2018	2018-2019
EVI	Max	0.70	0.59	0.91	0.80
EVI	Min	0.06	0.23	0.90	0.67
EVI	IntDry	0.55	0.64	0.89	0.34
NDMI	Max	0.38	0.42	0.58	0.38
NDMI	Min	0.57	0.09	0.98	0.45
NDMI	IntDry	0.17	0.18	0.76	0.33
NDVI	Max	0.07	0.59	0.46	0.051
NDVI	Min	0.89	**< 0.05**	0.56	0.38
NDVI	IntDry	**< 0.05**	0.13	0.40	0.51

Table 9 :P-values from multiple linear regression, conducted on only **dry forests** of **PRVI** for **AGLB net change** and max index, min index, and integral of the dry season for EVI, NDMI, and NDVI.

Index	Index Type	2010-2014	2016-2017	2017-2018	2018-2019
EVI	Max	0.50	0.66	0.98	0.13
EVI	Min	0.32	0.21	0.81	0.13
EVI	IntDry	0.74	0.55	0.87	0.19
NDMI	Max	0.76	0.41	0.65	0.29
NDMI	Min	0.21	0.14	0.44	0.14
NDMI	IntDry	0.90	0.30	0.32	**< 0.05**
NDVI	Max	0.84	0.29	0.34	0.12
NDVI	Min	0.34	0.08	0.38	**< 0.05**
NDVI	IntDry	0.67	0.33	0.11	0.18

Table 10: P-values from multiple linear regression, conducted on only **humid forests** of **PRVI** for **AGLB** and max index, min index, and integral of the dry season for EVI, NDMI, and NDVI.

Index	Index Type	2010-2014	2016-2017	2017-2018	2018-2019
EVI	Max	0.99	0.11	0.94	0.38
EVI	Min	**< 0.05**	0.47	0.91	0.80
EVI	IntDry	0.88	0.78	0.81	0.19
NDMI	Max	0.35	0.34	**< 0.05**	0.87
NDMI	Min	0.18	**< 0.05**	0.28	0.80
NDMI	IntDry	0.37	0.48	0.44	0.64
NDVI	Max	**< 0.05**	**< 0.05**	0.31	0.52
NDVI	Min	0.12	0.12	0.30	0.24
NDVI	IntDry	0.90	0.61	0.22	0.75

Table 11: P-values from multiple linear regression, conducted on only **humid forests** of **PRVI** for **AGLB net change** and max index, min index, and integral of the dry season for EVI, NDMI, and NDVI.

Index	Index Type	2010-2014	2016-2017	2017-2018	2018-2019
EVI	Max	0.62	0.59	0.84	0.69
EVI	Min	0.87	0.84	0.61	0.52
EVI	IntDry	0.87	0.42	0.60	0.68
NDMI	Max	0.51	0.31	0.89	0.15
NDMI	Min	0.72	0.11	0.72	0.63
NDMI	IntDry	0.77	0.42	0.86	0.79
NDVI	Max	0.49	0.47	0.29	0.08
NDVI	Min	0.82	0.65	0.50	0.73
NDVI	IntDry	0.80	0.22	0.81	0.40

Multiple linear regression was then rerun on only the main island's plots (Table 12 and 13). This reduced the analysis from four to only three time frames, as plots on the main island were not sampled during the 2018-2019 time frame. Results for AGLB remain relatively unchanged, while AGLB net change yielded no significant results. When the multiple linear regression was run on the main island's dry and humid forests separately, the majority of the significant p-values were found in humid forests (Table 14,

15, 16, and 17). Adjust R-squared values for all regression models ran again yielded only low values.

Table 12: P-values from multiple linear regression, conducted on **all forests** on the **Main Island** of Puerto Rico for **AGLB** and max index, min index, and integral of the dry season for EVI, NDMI, and NDVI.

Index	Index Type	2010-2014	2016-2017	2017-2018	2018-2019
EVI	Max	0.15	**< 0.05**	0.39	
EVI	Min	0.08	0.61	0.65	
EVI	IntDry	0.84	0.23	0.68	
NDMI	Max	0.131	0.20	**< 0.05**	
NDMI	Min	0.23	**< 0.05**	0.11	
NDMI	IntDry	0.86	0.09	0.06	
NDVI	Max	**< 0.05**	**< 0.05**	0.08	
NDVI	Min	0.65	0.43	0.15	
NDVI	IntDry	0.95	0.33	0.06	

Table 13: P-values from multiple linear regression, conducted on **all forests** on the **Main Island** of Puerto Rico for **AGLB net change** and max index, min index, and integral of the dry season for EVI, NDMI, and NDVI.

Index	Index Type	2010-2014	2016-2017	2017-2018	2018-2019
EVI	Max	0.27	0.64	0.83	
EVI	Min	0.95	0.94	0.66	
EVI	IntDry	0.98	0.35	0.55	
NDMI	Max	0.30	0.40	0.84	
NDMI	Min	0.88	0.14	0.68	
NDMI	IntDry	0.82	0.38	0.62	
NDVI	Max	0.32	0.89	0.46	
NDVI	Min	0.92	0.89	0.51	
NDVI	IntDry	0.80	0.39	0.50	

Table 14: P-values from multiple linear regression, conducted on only **dry forests** on the **Main Island** of Puerto Rico for **AGLB** and max index, min index, and integral of the dry season for EVI, NDMI, and NDVI.

Index	Index Type	2010-2014	2016-2017	2017-2018	2018-2019
EVI	Max	0.76	0.59	0.91	
EVI	Min	0.14	0.23	0.90	
EVI	IntDry	0.50	0.64	0.90	
NDMI	Max	0.50	0.43	0.58	
NDMI	Min	0.66	0.09	0.99	
NDMI	IntDry	0.80	0.18	0.76	
NDVI	Max	0.21	0.59	0.46	
NDVI	Min	0.65	**< 0.05**	0.56	
NDVI	IntDry	0.28	0.13	0.40	

Table 15: P-values from multiple linear regression, conducted on only **dry forests** on the **Main Island** of Puerto Rico for **AGLB net change** and max index, min index, and integral of the dry season for EVI, NDMI, and NDVI.

Index	Index Type	2010-2014	2016-2017	2017-2018	2018-2019
EVI	Max	0.32	0.66	0.98	
EVI	Min	0.58	0.21	0.81	
EVI	IntDry	0.92	0.55	0.87	
NDMI	Max	0.60	0.41	0.65	
NDMI	Min	0.94	0.14	0.44	
NDMI	IntDry	0.48	0.30	0.32	
NDVI	Max	0.75	0.29	0.34	
NDVI	Min	0.79	0.08	0.38	
NDVI	IntDry	0.84	0.33	0.11	

Table 16: P-values from multiple linear regression, conducted on only **humid forests** on the **Main Island** of Puerto Rico for **AGLB** and max index, min index, and integral of the dry season for EVI, NDMI, and NDVI.

Index	Index Type	2010-2014	2016-2017	2017-2018	2018-2019
EVI	Max	0.29	0.12	0.94	
EVI	Min	0.14	0.47	0.91	
EVI	IntDry	0.96	0.78	0.81	
NDMI	Max	0.06	0.30	**< 0.05**	
NDMI	Min	0.39	**< 0.05**	0.28	
NDMI	IntDry	0.95	0.36	0.44	
NDVI	Max	**< 0.05**	**< 0.05**	0.31	
NDVI	Min	0.51	0.12	0.30	
NDVI	IntDry	0.22	0.14	0.45	

Table 17: P-values from multiple linear regression, conducted on only **humid forests** on the **Main Island** of Puerto Rico for **AGLB net change** and max index, min index, and integral of the dry season for EVI, NDMI, and NDVI.

Index	Index Type	2010-2014	2016-2017	2017-2018	2018-2019
EVI	Max	0.33	0.59	0.84	
EVI	Min	0.73	0.84	0.61	
EVI	IntDry	0.78	0.42	0.60	
NDMI	Max	0.25	0.32	0.89	
NDMI	Min	0.90	0.11	0.72	
NDMI	IntDry	0.52	0.43	0.86	
NDVI	Max	0.34	0.47	0.29	
NDVI	Min	0.98	0.65	0.50	
NDVI	IntDry	0.88	0.30	0.22	

Simple linear regression was conducted on AGLB versus the Δ_{max} change of each spectral index. Regression yielded significant p-values for all indices; however, the low adjusted R-squared values indicate a weak relationship between the variables (Table 18 and 19). Data transformations were tested but did not yield better results.

Table 18: P-values from simple linear regression conducted on **all forests** for **AGLB** and the Δ_{max} index values for EVI, NDMI, and NDVI.

	Δ_{max} EVI	Δ_{max} NDMI	Δ_{max} NDVI
AGLB (PRVI)	**< 0.05**	**< 0.05**	**<0.05**
AGLB (only Main Island)	**< 0.05**	**< 0.05**	0.41

Table 19: Adjusted R^2 values from simple linear regression conducted on **all forests** for **AGLB** and the Δmax index values for EVI, NDMI, and NDVI.

	Δ_{max} EVI	Δ_{max} NDMI	Δ_{max} NDVI
AGLB (PRVI)	0.23	0.22	0.05
AGLB (only Main Island)	0.14	0.20	0.0

Mortality

Percent mortality was calculated for saplings, small trees, and large trees (Table 20). Overall, there was an increase in percent mortality in all categories after the hurricanes, which occurred between the 2016-2017 and 2017-2018 time frame. This trend is seen in the complete dataset, as well as when separated into dry and humid forests. Similar trends were also seen in percent mortality when analyzing only plots on the main island of Puerto Rico (Table 21). There was no data for the 2018-2019 time frame because no plots were surveyed on the main island during that time.

Table 20: Average **percent mortality** of **PRVI** for each time frame, additionally separated by **humid and dry forests**. Bold values indicate the percent mortality of all: both humid and dry forest combined.

	2010-2014	2016-2017	2017-2018	2018-2019
Sapling (All)	**19.7%**	**20.6%**	**24.7%**	**34.9%**
Sapling (Dry)	17.0%	15.4%	24.1%	37.0%
Sapling (Humid)	21.1%	21.7%	24.9%	33.0%
Small Tree (All)	**9.3%**	**9.1%**	**13.6%**	**16.8%**
Small Tree (Dry)	7.0%	6.9%	10.7%	10.7%
Small Tree (Humid)	10.4%	9.4%	14.1%	21.7%
Large Tree (All)	**5.6%**	**6.5%**	**16.6%**	**15.6%**
Large Tree (Dry)	0.0%	0.0%	20.0%	0.0%
Large Tree (Humid)	7.2%	7.5%	15.9%	20.0%

Table 21: Average **percent mortality** of only plots on the **Main Island** of Puerto Rico for each time frame, additionally separated by **humid and dry forests**. Bold values indicated the percent mortality of all both humid and dry forest combined.

	2010-2014	2016-2017	2017-2018	2018-2019
Sapling (All)	**22.3%**	**20.4%**	**28.9%**	
Sapling (Dry)	19.1%	14.6%	47.1%	
Sapling (Humid)	22.6%	21.0%	27.3%	
Small Tree (All)	**10.9%**	**10.0%**	**14.8%**	
Small Tree (Dry)	3.0%	9.9%	26.7%	
Small Tree (Humid)	11.6%	10.0%	13.8%	
Large Tree (All)	**8.7%**	**6.9%**	**19.6%**	
Large Tree (Dry)	0.0%	0.0%	50%	
Large Tree (Humid)	9.4%	7.7%	16.5%	

When conducting the Kruskal-Wallis Rank Sum Test on percent mortality by time frame, percent large tree mortality was significantly different among time frames for both forest types, and percent small tree mortality was significantly different among time frames for humid forest only (Table 22). However, when rerunning the test on only the main island's plots, none of the variables were significantly different (Table 23). I did not conduct the Dunn's test on mortality, since it did not show significant difference among groups, aside from large trees which showed significance by had a very small sample size.

Table 22: P-value results of Kruskal-Wallis Rank Sum Test on **PRVI** for **percent mortality** of saplings, small trees, and large trees.

	All Forests (Dry and Humid)	Dry Forests	Humid Forests
Saplings	0.11	0.18	0.53
Small Trees	0.08	0.93	**< 0.05**
Large Trees	**< 0.05**	**< 0.05**	**< 0.05**

Table 23: P-value results of Kruskal-Wallis Rank Sum Test on only the **Main Island** for **percent mortality** of saplings, small trees, and large trees.

	All Forests (Dry and Humid)	Dry Forests	Humid Forests
Saplings	0.20	0.18	0.43
Small Trees	0.45	0.85	0.41
Large Trees	0.07	0.12	0.10

Multiple linear regression was conducted on percent mortality (Table 24). Significant p-values were scattered among the time frames, such as significant values for NDVI max, min, and integral of the dry season with percent sapling mortality in 2016-2017, and minEVI and minNDMI with percent large tree mortality in 2010-2014. There were many significant p-values in the 2018-2019 time window, however they did not remain significant when the data was separated into humid and dry forests (Appendix E) or when the data was reduced to looking at just the main island of Puerto Rico (Appendix F, G). Between dry and humid forests, humid forests appeared to show more significance than dry. For all regression analysis that produced significant p-values, none produced any high adjusted R-squared values.

Table 24: P-values of multiple linear regression among time frames for the **percent mortality** saplings, small trees, and large trees, conducted on all **PRVI** plots.

Index	Variable	% Sap Mort (2010-2014)	% ST Mort (2010-2014)	% LT Mort (2010-2014)	% Sap Mort (2016-2017)	% ST Mort (2016-2017)	% LT Mort (2016-2017)	% Sap Mort (2017-2018)	% ST Mort (2017-2018)	% LT Mort (2017-2018)	% Sap Mort (2018-2019)	% ST Mort (2018-2019)	% LT Mort (2018-2019)
EVI	Max	0.34	0.54	0.58	0.30	0.38	0.88	0.98	0.27	0.40	0.29	0.06	0.29
EVI	Min	0.29	0.38	**< 0.05**	0.72	0.68	0.81	0.56	0.52	0.40	0.26	**< 0.05**	0.13
EVI	IntDry	0.46	0.45	0.65	0.26	0.71	0.80	0.79	0.86	0.11	0.06	**< 0.05**	0.09
NDMI	Max	0.93	0.83	0.07	0.85	0.10	0.99	0.27	0.16	0.38	0.48	**< 0.05**	0.19
NDMI	Min	0.80	0.48	0.1	0.45	0.07	0.92	0.86	0.28	0.27	0.23	**< 0.05**	0.12
NDMI	IntDry	0.84	0.27	0.98	0.77	0.10	0.79	0.81	0.17	0.08	**< 0.05**	**< 0.05**	0.07
NDVI	Max	0.50	0.90	0.44	**< 0.05**	0.23	0.08	0.39	0.84	0.56	0.51	0.09	0.90
NDVI	Min	0.71	0.39	**< 0.05**	**< 0.05**	0.58	0.11	0.51	0.76	0.54	0.21	**< 0.05**	0.73
NDVI	IntDry	0.66	0.87	0.70	**< 0.05**	0.79	0.75	0.71	0.76	0.13	**< 0.05**	0.62	0.23

Simple linear regression was additionally run to investigate the relationship between percent mortality and Δ_{max} index (Table 25 and 26). After running on PRVI and only the main island of Puerto Rico, no significant relationships were found.

Table 25: Results (p-values) from simple linear regression conducted on **PRVI's percent mortality** and the Δ_{max} index values for EVI, NDMI, and NDVI.

	% Sap Mort	% ST Mort	% LT Mort
Δ_{max} EVI	0.39	0.07	0.18
Δ_{max} NDMI	0.44	0.63	0.23
Δ_{max} NDVI	0.61	0.29	0.78

Table 26: Results (p-values) from simple linear regression conducted on only the **Main Island's percent mortality** and the Δmax index values for EVI, NDMI, and NDVI.

	% Sap Mort	% ST Mort	% LT Mort
Δ_{max} EVI	0.86	0.23	0.26
Δ_{max} NDMI	0.22	0.59	0.37
Δ_{max} NDVI	0.75	0.79	0.99

Phenology Curves

Phenology curves were generated for each index, visualizing the trends over 12 months. 2010-2014 and 2016-2017 were combined into one pre-hurricane curve (Figure 8). The values of the pre-hurricane time frames were weighted when combining, since 2010-2014 captures four years while 2016-2017 only captures one.

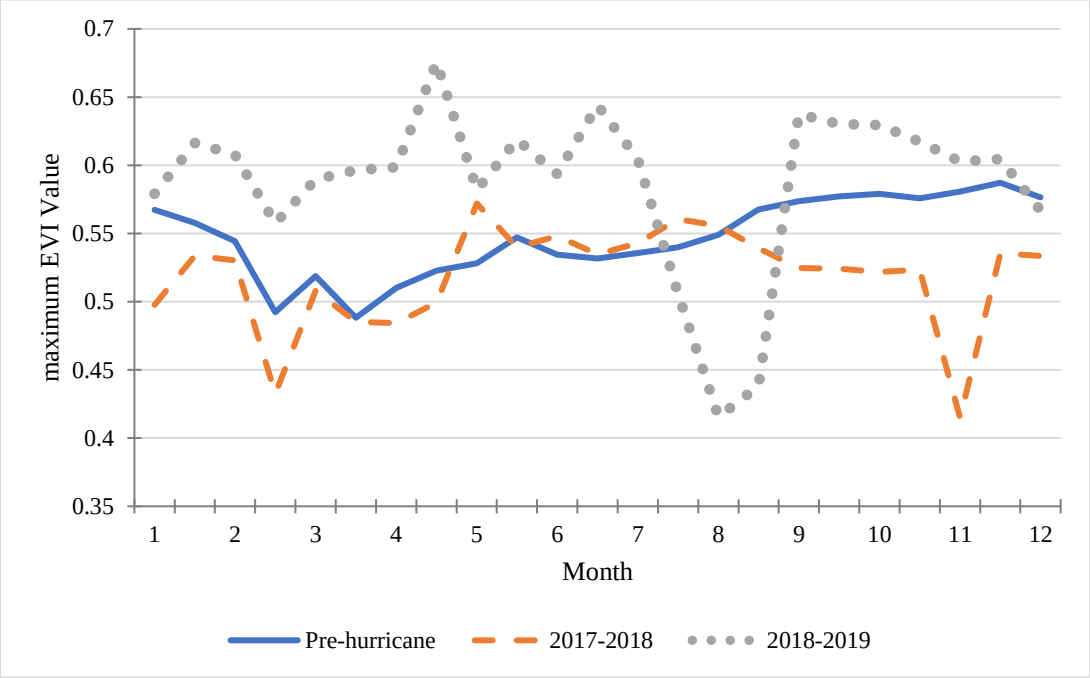

Figure 8: Phenology curves derived from FIA data showing EVI changes before and after the 2017 hurricanes. The x-axis in the months going across with 1 being January and 12 being December.

Phenology curves were also made using only plots from the island of Mona (Figure 9). This reduction in sample size focused in on a smaller area with more data availability and only one forest type, and thus produce more sound phenology curves.

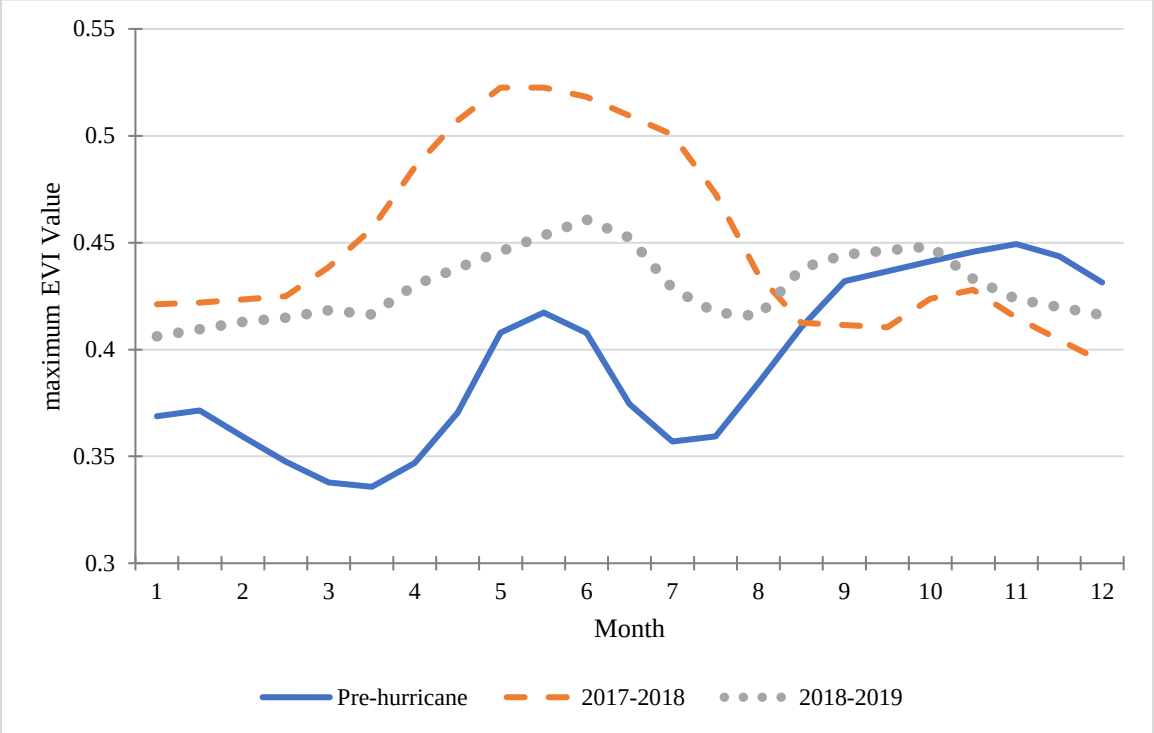

Figure 9: Phenology curves derived from FIA data, collected only from the island Mona, showing EVI changes before and after the 2017 hurricanes. The x-axis in the months going across with 1 being January and 12 being December.

DISCUSSION

This study showed that significant changes in tropical forests caused by hurricanes could be detected using remote sensing data. I was able to detect these trends by obtaining, processing, and producing near cloud-free imagery. Trends seen in the remote sensing data could also be seen in the FIA data. However, the inconsistency and scarcity in both the satellite data and the FIA data made it challenging to detect strong relationships between the datasets. These same challenges were present when generating phenology curves, but I was able to find more consistent trends when the study area was narrowed to a region with one forest type and no data gaps. Additionally, analysis further affirmed the necessity of more frequent field surveying to ground truth the remote sensing data.

Phenology Metrics

For the three spectral indices, I saw an initial drop in index values directly after the hurricane, followed but a spike in values the following year, especially in humid forests implying a sudden crash followed by a quick recovery (Figures 3, 4, and 5). It appears the first year after the hurricanes, the index values were low since the forests were stripped of their leaves, damaged, or killed, and therefore were producing less chlorophyll and taking in less moisture (Cox et al., 2019). However, in the second year post-hurricane (2018-2019) there was a spike in index values as the forests began to recover and regrow. This could be from new plants or species flourishing with a more

open canopy or from the surviving trees beginning to regrow, producing more chlorophyll, and taking in more water (Reed et al., 1994).

When conducting the Kruskal-Wallis Rank Sum Test on the spectral indices for all forests and when separated into dry and humid forests, all but 1 test, maxNDMI values for dry forest, showed significant differences among time frames. This was an indicator that these variables, which were generated using remotely sensed data, were able to detect on-the-ground forest changes. Results from Dunn's Test for Multiple Comparisons on the phenology metrics further emphasized the necessity for ground truthing when analyzing remote sensing data, as many of the results from these phenology metrics did not follow the same trends as the FIA data (Table 3). Some results contradicted trends that may have been expected, for instance maxNDMI for all forests shows significant different between its two pre-hurricane time frames (2010-2014 and 2016-2017) and significant difference between its two post-hurricane time frames (2017-2018 and 2018-2019), but no significant differences between some pre- and post-hurricane time frames (2010-2014 and 2017-2018, and 2016-2017 and 2018-2019). There was however, consistency among phenology metrics, i.e. the same time frames showing significant differences in one phenology metric were also significant for the other two metrics. These results also reaffirmed that more change was occurring in the humid forests, since most of the time frames for dry forests were not significantly different, but humid forests were.

Aboveground Live Biomass

Analyzing the boxplots of AGLB and AGLB net change showed there was a dramatic decrease, specifically in the humid forests, in the last two time frames (Figures 6 and 7). Since hurricanes are highly disruptive and destructive, a large decrease in AGLB and AGLB net change after the hurricanes was expected. The Kruskal-Wallis Rank Sum Test confirmed that these differences among time frames were significant.

When looking at AGLB and AGLB net change separated by forest type, a trend can be seen of humid forests having more variability among time frames than dry forests. When running the Kruskal-Wallis test on AGLB separated by forest type, only humid forests showed significant changes, further emphasizing that humid forests were more substantially altered among time frames. This could mean that humid forests or certain species within the humid forests are less resistant to environmental changes (Zimmerman et al., 1994; Lugo & Frangi, 2016).

Dunn's Test for Multiple Comparisons on AGLB and AGLB net change yielded many significant results. Looking at AGLB, time frame 4's humid forest (2018-2019) was significantly different from the other three time frames (Table 4). This matched the trends seen in the box plots, since we saw consistency in the 2 pre-hurricane time frames and little change in the first post-hurricane time frame, but a major drop in the 2nd post-hurricane time frame (Figure 6). AGLB net change's results also matched the trends visualized in the boxplots, as I found significant differences between the pre-hurricane time frames (2010-2014 and 2016-2017) and the post-hurricane time frames (2017-2018

and 2018-2019) (Figure 7, Table 5). Additionally, these results reaffirms that these were hurricane related changes, as there were no significant differences when comparing the two pre-hurricane periods with each another, and no significant differences when comparing the two post-hurricane periods with each other. Only significant differences were seen when comparing pre- and post-hurricane time frames.

Beyond both detecting significant change, I detected very few significant linear relationships between the FIA data and the remotely sensed data. Significant linear relationship that were detected explained very little variation in the data. When conducting multiple linear regression on both AGLB and AGLB net change versus the spectral indices, while I did see some significant p-values, adjusted R-squared values were low and overall, there were not any strong trends (Table 6 and 7). Breaking down the data to look at only dry forests or humid forest, or just the main island of Puerto Rico, did not yield any stronger results (Table 8, 9, 10, 11, 12, 13, 14, 15, 16, and 17).

When conducting simple linear regression, there were strong relationships detected from AGLB of saplings and Δ_{max} indices, however I hypothesize that there is no cause-and-effect relationship, but instead an association (Table 18 and 19). Despite many of the linear models having a significant p-value, the adjust R-squared values were relatively low, showing the data did not fit the regression line well. We can interpret this as high sapling biomass patches suffered most of the negative effects of the hurricanes, such as loss of vigor, as represented by the drop in mean EVI.

Mortality

While the increase in percent mortality can be seen in all three categories after the hurricanes, only large trees showed statistical significance (Table 22). This finding is likely attributed to lack of data, as the sample sizes for large trees were much smaller than the other two categories. Some plots had only 1 or 2 large trees, while others didn't have any. This makes the loss or survival of even a single large tree highly influential, and likely negates any significant findings.

Multiple linear regression on percent mortality and spectral indices did not yield any stronger results or trends (Table 24, Appendix E, F, G). This could mean that the on-the-ground changes occurring that were reflected in the FIA data may not be as easily detectable with the remote sensing data. This could be from the limitations of Landsat, such as its 30 by 30 meter spectral resolution or its 16 day return time (Zhang et al., 2009). It could also mean that the changes occurring are non-linear or more complex than the regression is able to show.

When conducting simple linear regression on percent mortality of saplings, small trees, and large trees, with the Δ_{max} index, I found no significant relationships (Table 25). I further isolated the data to only include plots located on the main island of Puerto Rico but still found no significant relationship (Table 26). When separating by habitat type, a linear relationship was only found in humid forests between percent mortality of small trees and a Δ_{max} EVI, albeit with a low R-squared value.

Phenology Curves

For the phenology curves, the extreme dips in the curves are due to the lack of data (Figure 8). Where these dips occurred, the only data available during that time frame was from the island of Mona and Southwestern Puerto Rico, or just Mona (Appendix A). This trend is expected, as the western regions of the island are more cloud-free, but also are largely dry forests with generally lower index values. Since data from these regions are the only ones available during those time frames, it is creating these dips that would normally be balanced and averaged out with other phenology data from around the island.

From generating phenology curves using only data from Mona, I produced meaningful curves (Figure 9). The two green ups and brown downs can be clearly seen in the pre-hurricane phenology curve, which was generated using the 2010-2014 and 2016-2017 time frames. In the pre-hurricane time frame the first green up was around mid-May (5^{th} and 6^{th} month), and the second, larger green up was from September to October (9^{th} to 11^{th} month). However, the 2017-2018 and 2018-2019 time frames produced quite difference curves. For these time frames I still had two green ups and two brown downs, but their timing was different. The post-hurricane time frames had their largest green up first, from mid-May to August (4^{th} to 7^{th} month), followed by a smaller green up around mid-October (10^{th} month). Another interesting trend we can see is right after the hurricane is the large increase in EVI values in both post-hurricane time windows. The values are significantly larger in the 2017–2018 time frame and then drop down in 2018-2019, closer to but still above the pre-hurricane curves.

The trend visualized in Mona phenology curves were different than the trends seen in boxplots for PRVI and the main island, which show that index values tended to drop in 2017-2018 directly after the hurricanes, then shoot up in 2018-2019 as the trees are greening up and recovering. However, these phenology curves are still very skewed due to the data gaps (missing time windows during the year when cloud cover was so bad that we could not use the images). These data gaps are causing the data from the very small island of Mona, which is only dry forests, to have a very strong influence on what is supposed to be phenology curves of the entire study site. Mona is not a strong representation of the entire island of Puerto Rico and the U.S. Virgin Islands. The phenology curves produced with only Mona's data should be only seen as representing Mona, and not assumed as a representation of all the islands. An alternative method for generating more meaningful phenology curves would be utilizing all the pixels across the islands, not just pixels that align with the FIA plots.

Exploratory Analysis

Since finding a significant relationship between the remote sensing data and FIA data proved to be challenging, I additionally singled out the EVI for humid forests dataset to generate scatterplots to see if I could find any other interesting trends and patterns. EVI for humid forests was selected to investigate because it was the dataset with the most significant p-values.

The range of the data in the pre-hurricane time frames stayed relatively consistent. In the 2010-2014 time frame, most points fell between an EVI value of 0.5 and 0.8 and

between 0 and 200 AGLB in mg/ha (Figure 10-A). In the 2016-2017 time frame, most points fell between an EVI value of 0.55 and 0.85, slightly higher than the previous time frame, but stayed between 0 and 200 for AGLB in mg/ha (Figure 10-B). In the two post-hurricane time frames, the range of the data changed. In the 2017-2018 time frame, most points fell between an EVI value of 0.55 and 0.75 and between 0 and 200 AGLB in mg/ha (Figure 10-C). In the 2018-2019 time frame, most points fell between an EVI value of 0.7 and 0.9, but between 0 and 100 AGLB in mg/ha (Figure 10-D). While the EVI values appear to increase, the amount of AGLB dropped significantly by roughly half.

In the prehurricane time frames the trend lines have a slightly positive trend. While the R-squared values for these time frames were very low, it is interesting and noteworthy that both had a similar trend that explain roughly 5% of variation in the data. These were also the two time frames with the most FIA plots, with 223 plots for 2010-2014 and 96 plots for 2016-2017. Although a high R-squared values is generally desired, perhaps 5% variation is all that can be explained using phenology metrics for forested areas with dense canopy cover (Pettorelli et al., 2005).

In the two post-hurricane time frames, there is almost a straight trend line in the 2017-2018 time frame, and a slightly negative trend line in the 2018-2019 time frame. The post-hurricane time frames do not have as many FIA plots as the pre-hurricane time frame, with 37 plots in the 2017-2018 time frame and 23 plots in the 2018-2019 time frame. Because of this scarcity of data it is difficult to see as clear shapes or trends in the data.

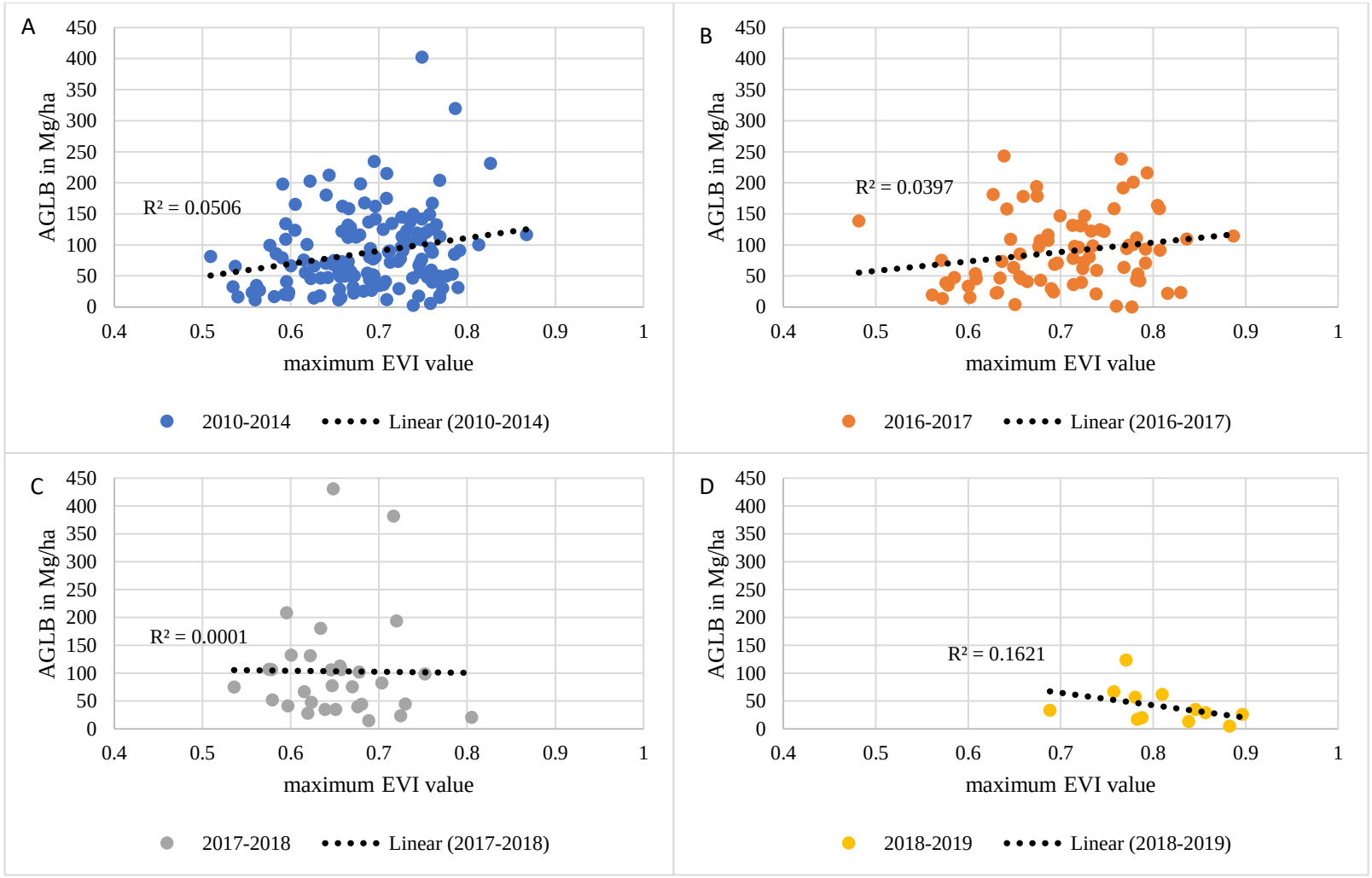

Figure 10: Scatterplots showing linear models for **PRVI's Humid Forest** for each time frame for **AGLB** in Mg/ha on the y axis and maximum EVI value on the x axis. The black dotted line shows the best trend line.

When looking all the FIA plots for every time frame on the scatter plot, we can see there is no obvious linear trends (Figure 11). Points generally are not lower than an EVI value of 0.55 and fan out into a megaphone shape as EVI increases. Most of the points fall between an EVI value of 0.6 and 0.8 and an AGLB value of 0 and 200 Mg/ha.

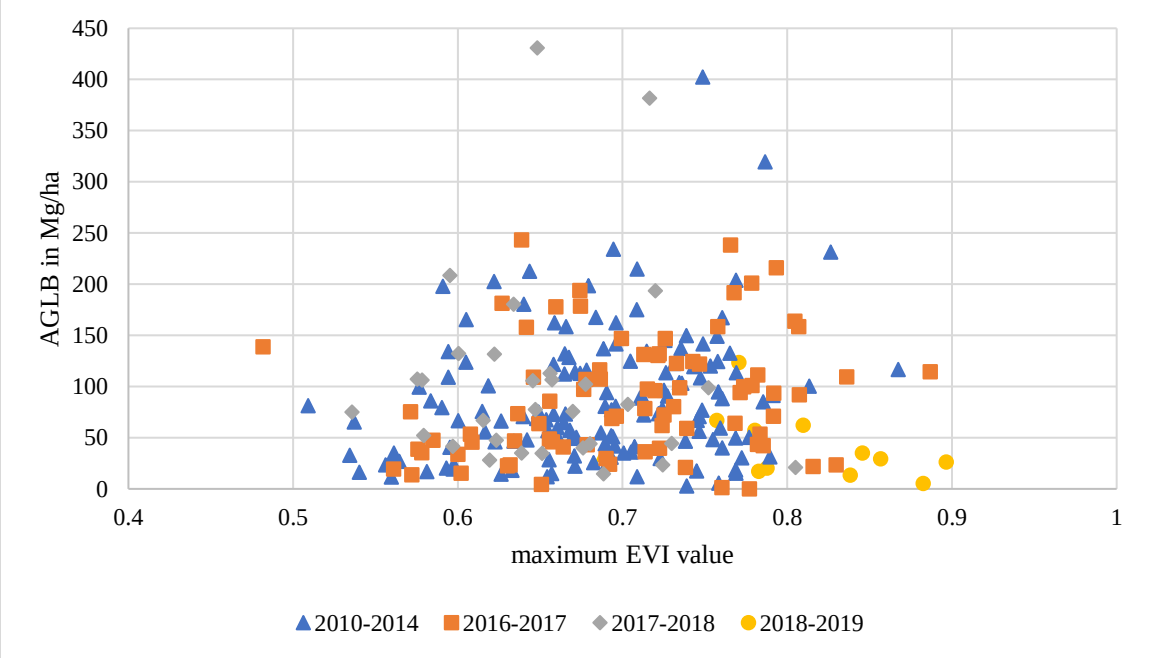

Figure 11: Scatterplot showing a linear model of **PRVI's Humid Forests** all time frames for aboveground live biomass in mg/ha on the y axis and maximum EVI value on the x axis. The black dotted line shows the best trend line.

These results emphasize the demand for more frequent ground surveying. Ideally, we would want surveying of the same set of plots twice a month, in line with when Landsat imagery is being taken. More frequent surveys would fill in the post-hurricane scatter plots and better visualize the changes occurring. This would also help confirm if the trend being seen of 5% variation explained held true in the post-hurricanes time periods, or if the hurricanes altered this pattern.

Uncertainties

In the mortality data, AGLB data, and phenology data the effects of the hurricane can be visually seen. For mortality, I saw an increase in percent mortality in sapling, small trees, and large trees after the hurricanes. For AGLB, there was a decrease in Mg/ha after the hurricanes. For AGLB net change, there was a drop directly after the hurricanes, followed by an increase as the plants begin to recover 1 year later. For phenology data, in all indices there was an initial drop in index values in the 2017-2018 time frame after the hurricane, followed by a spike in index value the following year, even higher than pre-hurricane values, as the forest was recovering.

These changes were also verified using the Kruskal-Wallis Rank Sum Test, confirming that there was significant change among the time frame, indicating the hurricanes caused significant, detectable change. However, beyond identifying significant change, I was not able to identify any linear relationships that linked the satellite derived phenology metrics to the on the ground FIA data. This could be for a variety of reasons of reasons, such as preprocessing errors or differences in sampling of on the ground plots. Another factor to consider is that these are dense tropical forests, and Landsat has a 30 x 30 meters pixel size and only captures the top of the canopy. Because of this, it does not detect understory trees, shrubs, or any other complexity that lies underneath the canopy (Zhang et al., 2009). Additionally, EVI and NDVI are vegetation indices and NDMI is a moisture index, i.e., only proxies for biomass (Santin-Janin et al., 2009). Because of this we may often find discrepancies in our results, as large trees being destroyed and

replaced with new, small trees would yield smaller AGLB values, but would likely show a high EVI and NDVI values as there is a lot of plant growth being detected (Gaw & Richards, 2021). Trees also grow rapidly when they are young, which could have contributed to the sharp increase in index values in the last time frame as new growth is booming.

CONCLUSIONS AND RECOMMENDATIONS

This study demonstrated the ability and challenges of Earth observations to detect the effects of climatic anomalies across a tropical landscape. I demonstrated a novel approach to detecting and removing cloud cover using ENVI and IDL. This method allowed for the reconstruction of time series images through a series of codes and processes. With the increase in climatic anomalies as climate change intensifies, I believe this methodology will provide a solid baseline for remote tropical forest phenology detection and allow for future work and expansion.

The goals of this study were to evaluate the effects of the hurricanes on aboveground live biomass and tree mortality and to detect trends in relation to changes in phenological metrics. While I was able to detect substantial changes that occurred in AGLB and percent mortality after the hurricanes, substantial trends and relationships with remote sensing indices were either weak or not detectable.

In this study, phenology curves were generated for visual interpretation. Further research could examine temporal curves from these indices to summarize phenological stages, create mean phenology variables utilizing similarities among years, and find patterns indicative of forest characteristics. Anomalies could also be quantified by determining the deviation of phenology matrices between the post disturbance periods (2017-2018 and 2018-2019) and the normal, undisturbed periods (2010-2014 and 2016-2017). These deviations could be used to link climate and vegetation and thus examine mortality and growth in relation to future change. Additionally, while I only looked at dry

and humid forests, the humid forests can be further divided into 5 different types: subtropical moist, subtropical rain, lower montane rain, lower montane wet, and subtropical wet forests (Miller & Lugo, 2009). Future analysis could be conducted on these humid forest types since I found more accuracy when looking at just the dry forests alone.

One of the primary conclusions from this analysis is the phenology and forest changes relationship is more complex than a linear relationship could explain, or that the data or analyses are not robust enough to detect it. Future studies may find value in incorporating additional factors such as species diversity, forest type beyond just dry and humid, landscape elements such as slope, aspect, and elevation, and climatic variables such as precipitation, temperature, and hurricane path. Incorporating other sources of on-the-ground data, similar to FIA but with consistent, more frequent resampling could also aid in further studies. Adding in other satellite imagery such as Sentinel, MODIS, or imagery from high resolution private satellites may also be of value. Another avenue to be explored would be conducting patch analysis on FIA data and grouping plots together based on region and index range to better identify anomalies. Tropical forests are complex ecosystems and looking at these variables may yield insightful results. The data has provided useful information for researchers using Earth observation to detect climatic changes and can be used in future remote sensing and climate related studies.

LITERATURE CITED

Asner, G. P., Townsend, A. R., & Braswell, B. H. (2000). Phenology and Productivity. *Geophysical Research Letters*, *27*(7), 981–984.

Boose, E. R., Serrano, M. I., & Foster, D. R. (2004). Landscape and regional impacts of hurricanes in Puerto Rico. *Ecological Monographs*, *74*(2), 335–352. doi:10.1890/02-4057

Brokaw, N. V. L., & Grear, J. S. (1991). Forest Structure Before and After Hurricane Hugo at Three Elevations in the Luquillo Mountains, Puerto Rico. *Biotropica*, *23*(4a), 386–392.

Burrill, E., Wilson, A. M., Turner, J., Pugh, S., Menlove, J., Christiansen, G., Conkling, B., & David, W. (2018). *The Forest Inventory and Analysis Database: database description and user guide version 8.0 for Phase 2*. http://www.fia.fs.fed.us/library/database-documentation/

Chen, X., & Pan, W. (2002). Relationships among phenological growing season, time-integrated normalized difference vegetation index and climate forcing in the temperature region of Eastern China. *International Journal of Climatology*, *22*(14), 1781–1792. doi:10.1002/joc.823

Cox, D., Arikawa, T., Barbosa, A., Guannel, G., Inazu, D., Kennedy, A., Li, Y., Mori, N., Perry, K., Prevatt, D., Roueche, D., Shimozono, T., Simpson, C., Shimakawa, E., Shimura, T., & Slocum, R. (2019). Hurricanes Irma and Maria post-event survey in US Virgin Islands. *Coastal Engineering Journal*, *61*(2), 121–134. doi:10.1080/21664250.2018.1558920

Dinno, A. (2015). Nonparametric pairwise multiple comparisons in independent groups using Dunn's test. *Stata Journal*, *15*(1), 292–300. doi:10.1177/1536867x1501500117

Emanuel, K. (2003). Tropical Cyclones. *Annual Review of Earth and Planetary Sciences*, *31*(1), 75–104. https://doi.org/10.1146/annurev.earth.31.100901.141259

Ewel, J. J., & Whitmore, J. L. (1973). The ecological life zones of Puerto Rico and the U.S.Virgin Islands. *Forest Service Research Paper ITF-18*. doi:10.1017/CBO9781107415324.004

Francis, J. K., & Liogier, H. A. (1991). Naturalized Exotic Tree Species in Puerto Rico. *United States Department of Agriculture*, General Technical Report (SO-82).

Gardner, T. A., Barlow, J., Chazdon, R., Ewers, R. M., Harvey, C. A., Peres, C. A., & Sodhi, N. S. (2009). Prospects for tropical forest biodiversity in a human-modified world. *Ecology Letters 12*(6) 561–582. doi:10.1111/j.1461-0248.2009.01294.x

Gaw, L. Y. F., & Richards, D. R. (2021). Development of spontaneous vegetation on reclaimed land in Singapore measured by NDVI. *PLoS ONE*, *16*(1), 1–16. doi.org:/10.1371/journal.pone.0245220

Goetz, A. F. H., Rock, B. N., & Rowan, L. C. (1983). Remote sensing for exploration: an overview. *Economic Geology*, *78*(4), 573–590. doi:10.2113/gsecongeo.78.4.573

Gray, E. (2018). *NASA Provides New Look at Puerto Rico Post-Hurricane Maria*. https://www.nasa.gov/feature/goddard/2018/nasa-provides-new-look-at-puerto-rico-post-hurricane-maria

Gwenzi, D., Helmer, E., Zhu, X., Lefsky, M., & Marcano-Vega, H. (2017). Predictions of Tropical Forest Biomass and Biomass Growth Based on Stand Height or Canopy Area Are Improved by Landsat-Scale Phenology across Puerto Rico and the U.S. Virgin Islands. *Remote Sensing*, *9*(2), 123. doi:10.3390/rs9020123

Hecke, T. Van. (2012). Power study of anova versus Kruskal-Wallis test. *Journal of Statistics and Management Systems*, *15*(2–3), 241–247. doi:10.1080/09720510.2012.10701623

Helmer, E. H., Kennaway, T. A., Pedreros, D. H., Clark, M. L., Marcano-Vega, H., Tieszen, L. L., Ruzycki, T. R., Schill, S. R., & Carrington, C. M. S. (2008). Land Cover and Forest Formation Distributions for St. Kitts, Nevis, St. Eustatius, Grenada and Barbados from Decision Tree Classification of Cloud-Cleared Satellite Imagery. *Caribbean Journal of Science, 44(*2), 175-198.

Helmer, E. H., Ruzycki, T. S., Wilson, B. T., Sherrill, K. R., Lefsky, M. A., Marcano-Vega, H., Brandeis, T. J., Erickson, H. E., & Ruefenacht, B. (2018). Tropical Deforestation and Recolonization by Exotic and Native Trees: Spatial Patterns of Tropical Forest Biomass, Functional Groups, and Species Counts and Links to Stand Age, Geoclimate, and Sustainability Goals. *Remote Sensing*, *10*(11). doi:10.3390/rs10111724

Hilibrand, A. S., & Robbins, M. (2004). NASA strategic plan. *The Spine Journal*, *4*, 190S-194S. https://www.nasa.gov/sites/default/files/files/FY2014_NASA_SP_508c.pdf

Horion, S., Fensholt, R., Tagesson, T., & Ehammer, A. (2014). Using earth observation-based dry season NDVI trends for assessment of changes in tree cover in the Sahel. *International Journal of Remote Sensing*, *35*(7), 2493–2515. doi:10.1080/01431161.2014.883104

Isbell, F., Craven, D., Connolly, J., Loreau, M., Schmid, B., Beierkuhnlein, C., Bezemer, T. M., Bonin, C., Bruelheide, H., De Luca, E., Ebeling, A., Griffin, J. N., Guo, Q., Hautier, Y., Hector, A., Jentsch, A., Kreyling, J., Lanta, V., Manning, P., … Eisenhauer, N. (2015). Biodiversity increases the resistance of ecosystem productivity to climate extremes. *Nature*, *526*(7574), 574–577. doi:10.1038/nature15374

Jackson, R. D. (1983). Spectral indices in N-Space. *Remote Sensing of Environment, 13*(5), 409–421. doi:10.1016/0034-4257(83)90010-X

Kramer, K., Leinonen, I., & Loustau, D. (2000). The importance of phenology for the evaluation of impact of climate change on growth of boreal, temperate and Mediterranean forests ecosystems: An overview. *International Journal of Biometeorology, 44*(2), 67–75. doi:10.1007/s004840000066

LaMorte, W. (2016). Multivariate Methods. *Boston University School of Public Health: Multivariable Methods*. https://sphweb.bumc.bu.edu/otlt/mph-modules/bs/bs704-ep713_multivariablemethods/bs704-ep713_multivariablemethods2.html

Lieberman, D. (1982). Seasonality and Phenology in a Dry Tropical Forest in Ghana. *Journal of Ecology, 70,* 791-806.

Lugo, A. E., & Likens, G. E. (1992). Hurricane Hugo: Damage to a tropical rain forest in Puerto Rico. *Journal of Tropical Ecology*, *8*(1), 47–55. doi.org:10.1017/S0266467400006076

Lugo, A. E., & Frangi, J. L. (2016). Long-term response of Caribbean palm forests to hurricanes. *Caribbean Naturalist, 1*, 157–175.

Mann, M. E., & Emanuel, K. A. (2006). Atlantic Hurricane trends linked to climate change. *Eos, 87*(24), 233–235. https://doi.org/10.1029/2006EO240001

Miller, G. L., & Lugo, A. E. (2009). Guide to the ecological systems of Puerto Rico. *United States Department of Agriculture*. General Technical Report (IITF-GTR-35)

Ostertag, R., Silver, W. L., & Lugo, A. E. (2005). Factors affecting mortality and resistance to damage following hurricanes in a rehabilitated subtropical moist forest. *Biotropica*, *37*(1), 16–24. doi:10.1111/j.1744-7429.2005.04052.x

Parés-Ramos, I. K., Gould, W. A., & Aide, T. M. (2008). Agricultural Abandonment, Suburban Growth, and Forest Expansion in Puerto Rico between 1991 and 2000. *Ecology and Society 13*(2).

Pettorelli, N., Vik, J. O., Mysterud, A., Gaillard, J. M., Tucker, C. J., & Stenseth, N. C. (2005). Using the satellite-derived NDVI to assess ecological responses to environmental change. *Trends in Ecology and Evolution*, *20*(9), 503–510. doi:10.1016/j.tree.2005.05.011

Reed, B. C., Brown, J. F., VanderZee, D., Loveland, T. R., Merchant, J. W., & Ohlen, D. O. (1994). Measuring phenological variability from satellite imagery. *Journal of Vegetation Science, 5*(5), 703–714. doi:10.2307/3235884

Richards, J. A., & Jia, X. (2006). Remote sensing digital image analysis: An introduction. In *Remote Sensing Digital Image Analysis: An Introduction*. https://doi.org/10.1007/3-540-29711-1

Roy, D. P., Zhang, H. K., Ju, J., Gomez-Dans, J. L., Lewis, P. E., Schaaf, C. B., Sun, Q.,

Li, J., Huang, H., & Kovalskyy, V. (2016). A general method to normalize Landsat reflectance data to nadir BRDF adjusted reflectance. *Remote Sensing of Environment*, *176*, 255–271. doi:10.1016/j.rse.2016.01.023

Rudel, T. K., Perez-Lugo, M., & Zichal, H. (2000). When Fields Revert to Forest: Development and Spontaneous Reforestation in Post-War Puerto Rico. *Professional Geographer*, *52*(3), 386–397. doi:10.1111/0033-0124.00233

Santin-Janin, H., Garel, M., Chapuis, J. L., & Pontier, D. (2009). Assessing the performance of NDVI as a proxy for plant biomass using non-linear models: A case study on the kerguelen archipelago. *Polar Biology*, *32*(6), 861–871. doi:10.1007/s00300-009-0586-5

Thompson, I., Mackey, B., McNulty, S., & Mosseler, A. (2009). Forest Resilience, Biodiversity, and Climate Change: a synthesis of the biodiversity/resilience/stability relationship in forest ecosystems. Secretariat of the Convention on Biological Diversity, Montreal. Technical Series no. 43. In *Secretariat of the Convention on Biological Diversity.* (Vol. 43).

Tian, X., & Zou, X. (2018). Capturing size and intensity changes of hurricanes Irma and Maria (2017) from polar-orbiting satellite microwave radiometers. *Journal of the Atmospheric Sciences*, *75*(8), 2509–2522. doi:10.1175/JAS-D-17-0315.1

USDA. (2014). *The Forest Inventory and Analysis Database Description*. *2*, 748 pgs. https://www.fia.fs.fed.us/library/database-documentation/historic/ver6/FIADB User Guide P2_6-0-1_final.pdf%0Ahttp://www.fia.fs.fed.us/library/database-documentation/

Wang, C., Chen, J., Wu, J., Tang, Y., Shi, P., Black, T. A., & Zhu, K. (2017a). A snow-free vegetation index for improved monitoring of vegetation spring green-up date in deciduous ecosystems. *Remote Sensing of Environment*, *196*, 1–12. doi:10.1016/j.rse.2017.04.031

Wang, C., Chen, J., Wu, J., Tang, Y., Shi, P., Black, T. A., & Zhu, K. (2017b). A snow-free vegetation index for improved monitoring of vegetation spring green-up date in deciduous ecosystems. *Remote Sensing of Environment*, *196*, 1–12. doi:10.1016/j.rse.2017.04.031

Wei, H., Heilman, P., Qi, J., Nearing, M. A., Gu, Z., & Zhang, Y. (2012). Assessing phenological change in China from 1982 to 2006 using AVHRR imagery. *Frontiers of Earth Science*, *6*(3), 227–236. doi:10.1007/s11707-012-0321-3

Williams, D. L., Goward, S., & Arvidson, T. (2006). Landsat : Yesterday , Today , and Tomorrow. *Photogrammetric Engineering & Remote Sensing 72*(10), 1171–1178.

Zhang, X., Friedl, M. A., & Schaaf, C. B. (2009). Sensitivity of vegetation phenology detection to the temporal resolution of satellite data. *International Journal of Remote Sensing*, *30*(8), 2061–2074. doi:10.1080/01431160802549237

Zhu, X., Gao, F., Liu, D., & Chen, J. (2012). A modified neighborhood similar pixel interpolator approach for removing thick clouds in landsat images. *IEEE Geoscience and Remote Sensing Letters*, *9*(3), 521–525. doi:10.1109/LGRS.2011.2173290

Zhu, X., & Helmer, E. H. (2018). An automatic method for screening clouds and cloud shadows in optical satellite image time series in cloudy regions. *Remote Sensing of Environment*, *214*, 135–153. doi:10.1016/j.rse.2018.05.024

Zhu, X., Helmer, E. H., Chen, J., & Liu, D. (2019). An Automatic System for Reconstructing High-Quality Seasonal Landsat Time Series. *Remote Sensing Time Series Image Processing*, *2*, 25–42. doi:10.1201/9781315166636-2

Zimmerman, J. K., Everham. E. M., III, Waide, R. B., Lodge, D. J., Taylor, C. M., & Brokaw, N. V. L. (1994). Responses of Tree Species to Hurricane Winds in Subtropical Wet Forest in Puerto Rico: Implications for Tropical Tree Life Histories. *The Journal of Ecology*, *82*(4), 911. doi:10.2307/2261454

APPENDICES

Appendix A: Maps showing Forest Inventory and Analysis (FIA) plot locations on PRVI during each time frame.

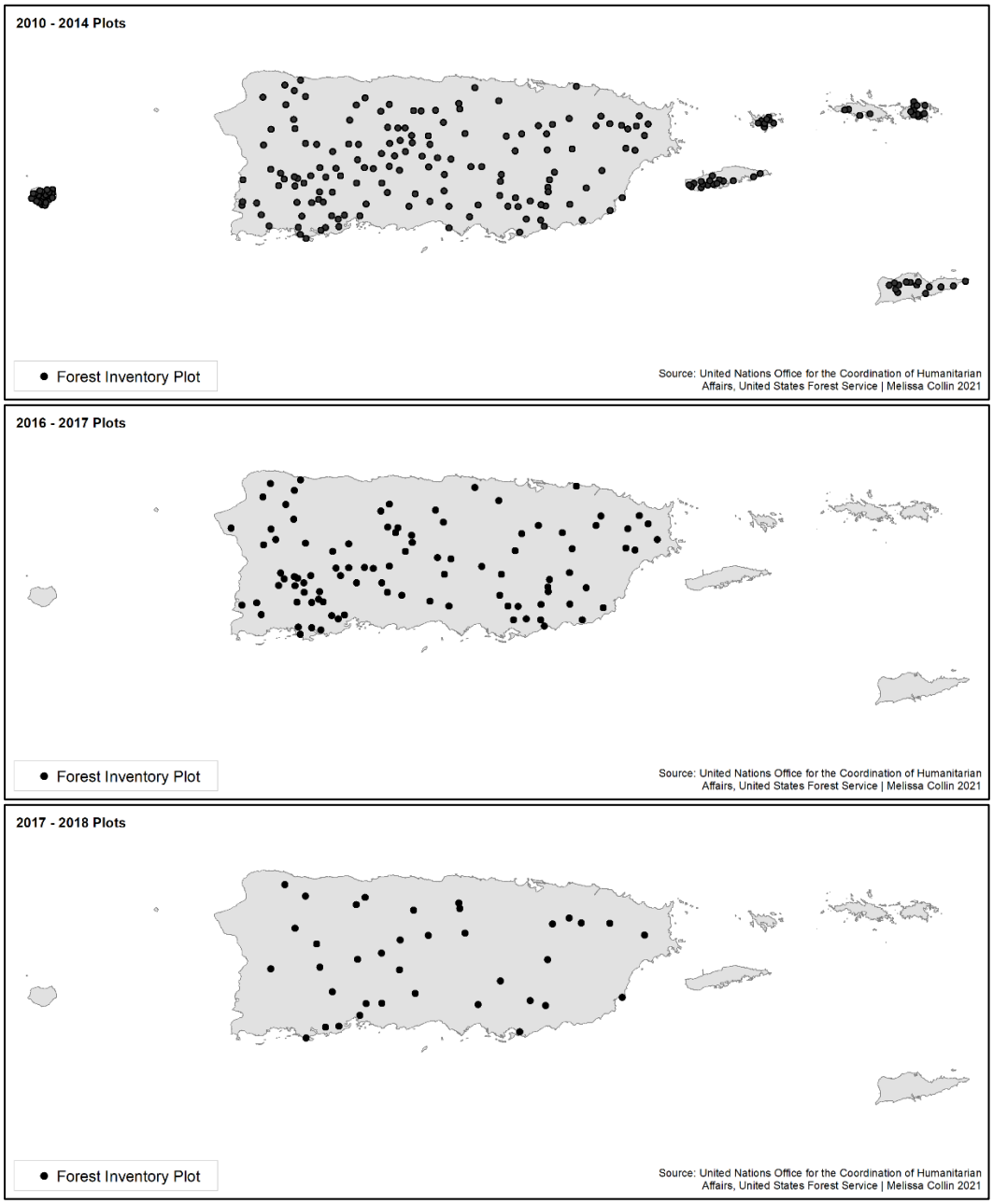

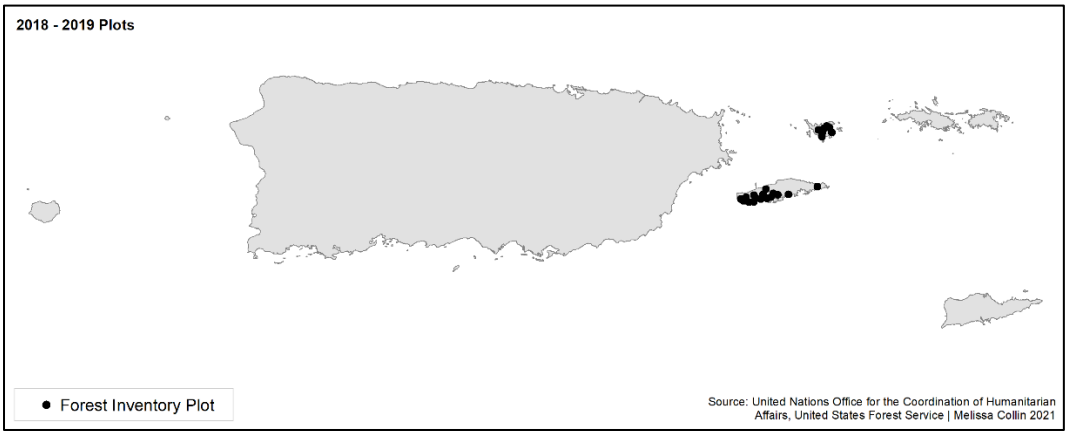
2018 - 2019 Plots
Forest Inventory Plot
Source: United Nations Office for the Coordination of Humanitarian Affairs, United States Forest Service | Melissa Collin 2021

Appendix B: Number of FIA plots sampled for mortality in each region for each time frame. There's a combined total of 358 plots, 264 of which were sampled on the main island of Puerto Rico.

Region (abbrev.)	2010-14	2016-17	2017-18	2018-19	Total
Northwest and Central Puerto Rico (Main)	101	61	26		188
Northeast Puerto Rico (NEMain)	13	11	3		27
Southeast Puerto Rico (SEMain)	6	4			10
Southwest Puerto Rico (SW)	20	14	5		39
Mona (Mona)	25				25
Vieques (NE1)	14			15	29
Culebra (NE2)	7			6	13
St Croix (SE1)	12				12
St Thomas and St John (NE3)	15				15
Total	213	90	34	21	358

Appendix C: Results of Dunn's Test on phenology metrics for **dry forests** in **PRVI**. Comparison columns indicates the two time frames being compared (1 = 2010-2014, 2 = 2016-2017, 3 = 2017-2018, 4 = 2018-2019). Pre-hurricane time frames are in orange and post-hurricane time frames are in blue. An adjusted p-value (P. adj) of <0.05 indicates the two time frames being compared are significantly different from each other.

Index Type	Comparison 1 (EVI)	Comparison 2 (EVI)	P. adj (EVI)	Comparison 1 (NDMI)	Comparison 2 (NDMI)	P. adj (NDMI)	Comparison 1 (NDVI)	Comparison 2 (NDVI)	P. adj (NDVI)
Max	1	2	0.30	1	2	0.65	1	2	0.06
Max	1	3	1.00	1	3	1.00	1	3	1.00
Max	2	3	0.39	2	3	1.00	2	3	1.00
Max	1	4	0.46	1	4	1.00	1	4	0.14
Max	2	4	1.00	2	4	1.00	2	4	1.00
Max	3	4	0.42	3	4	1.00	3	4	1.00
Min	1	2	0.07	1	2	0.15	1	2	<0.05
Min	1	3	0.72	1	3	0.21	1	3	0.26
Min	2	3	1.00	2	3	1.00	2	3	1.00
Min	1	4	<0.05	1	4	0.08	1	4	<0.05
Min	2	4	1.00	2	4	1.00	2	4	1.00
Min	3	4	1.00	3	4	1.00	3	4	1.00
IntDry	1	2	1.00	1	2	<0.05	1	2	<0.05
IntDry	1	3	0.16	1	3	1.00	1	3	<0.05
IntDry	2	3	1.00	2	3	1.00	2	3	1.00
IntDry	1	4	<0.05	1	4	<0.05	1	4	<0.05
IntDry	2	4	<0.05	2	4	<0.05	2	4	<0.05
IntDry	3	4	1.00	3	4	<0.05	3	4	<0.05

Appendix D: Results of Dunn's Test on phenology metrics for **humid forests** in **PRVI**. Comparison columns indicates the two time frames being compared (1 = 2010-2014, 2 = 2016-2017, 3 = 2017-2018, 4 = 2018-2019). Pre-hurricane time frames are in orange and post-hurricane time frames are in blue. An adjusted p-value (P. adj) of <0.05 indicates the two time frames being compared are significantly different from each other.

Index Type	Comparison 1 (EVI)	Comparison 2 (EVI)	P. adj (EVI)	Comparison 1 (NDMI)	Comparison 2 (NDMI)	P. adj (NDMI)	Comparison 1 (NDVI)	Comparison 2 (NDVI)	P. adj (NDVI)
Max	1	2	<0.05	1	2	<0.05	1	2	<0.05
Max	1	3	<0.05	1	3	<0.05	1	3	<0.05
Max	2	3	<0.05	2	3	<0.05	2	3	<0.05
Max	1	4	<0.05	1	4	<0.05	1	4	<0.05
Max	2	4	<0.05	2	4	<0.05	2	4	<0.05
Max	3	4	<0.05	3	4	<0.05	3	4	<0.05
Min	1	2	<0.05	1	2	<0.05	1	2	<0.05
Min	1	3	<0.05	1	3	<0.05	1	3	<0.05
Min	2	3	<0.05	2	3	<0.05	2	3	<0.05
Min	1	4	<0.05	1	4	<0.05	1	4	<0.05
Min	2	4	<0.05	2	4	1.00	2	4	1.00
Min	3	4	<0.05	3	4	<0.05	3	4	<0.05
IntDry	1	2	1.00	1	2	<0.05	1	2	<0.05
IntDry	1	3	<0.05	1	3	<0.05	1	3	<0.05
IntDry	2	3	<0.05	2	3	<0.05	2	3	<0.05
IntDry	1	4	1.00	1	4	<0.05	1	4	<0.05
IntDry	2	4	1.00	2	4	1.00	2	4	1.00
IntDry	3	4	<0.05	3	4	<0.05	3	4	<0.05

Appendix E: P-values of Multiple linear regression between time frames on the percent mortality saplings, small trees, and large trees, conducted on **dry forests and humid forests** on all **PRVI plots**. Bold indicates a significant p-value of less than 0.05.

Index	Band	Habitat Type	% Sap Mort (2010-2014)	% ST Mort (2010-2014)	% LT Mort (2010-2014)	% Sap Mort (2016-2017)	% ST Mort (2016-2017)	% LT Mort (2016-2017)	% Sap Mort (2017-2018)	% ST Mort (2017-2018)	% LT Mort (2017-2018)	% Sap Mort (2018-2019)	% ST Mort (2018-2019)	% LT Mort (2018-2019)
EVI	Max	Dry	0.99	0.52	NA	0.12	0.09	NA	0.75	0.85	0.87	0.89	**< 0.05**	NA
EVI	Min	Dry	0.57	0.55	NA	0.08	0.20	NA	0.91	0.99	0.98	1	**< 0.05**	NA
EVI	IntDry	Dry	0.42	0.12	NA	0.31	0.37	0	0.49	0.70	0.73	0.51	**< 0.05**	NA
NDMI	Max	Dry	0.58	0.17	NA	0.44	0.82	NA	0.94	NA	NA	0.26	0.19	NA
NDMI	Min	Dry	0.52	0.34	NA	0.33	0.69	NA	0.55	NA	NA	0.18	0.07	NA
NDMI	IntDry	Dry	0.86	0.77	NA	0.20	0.57	NA	0.46	NA	NA	0.23	0.06	NA
NDVI	Max	Dry	0.39	0.17	NA	0.15	0.98	NA	0.89	0.63	0.60	0.2	0.26	NA
NDVI	Min	Dry	0.16	0.65	NA	0.21	0.82	NA	0.85	0.65	0.64	0.10	**< 0.05**	NA
NDVI	IntDry	Dry	0.86	0.49	NA	0.26	0.36	NA	0.50	0.46	0.42	0.45	0.36	0
EVI	Max	Humid	0.85	0.10	0.73	0.26	0.75	0.71	0.50	0.36	0.22	0.30	0.66	0.18
EVI	Min	Humid	0.32	0.46	0.06	0.48	0.89	0.86	0.37	0.62	0.18	0.20	0.06	0.06
EVI	IntDry	Humid	0.60	0.76	0.86	0.35	0.88	0.52	0.67	0.86	0.35	0.09	0.17	0.06
NDMI	Max	Humid	0.18	**< 0.05**	0.21	0.82	**< 0.05**	0.85	0.34	0.22	0.53	0.23	0.41	0.23
NDMI	Min	Humid	0.93	0.49	0.17	0.53	**< 0.05**	0.32	0.71	0.47	0.81	0.79	0.70	0.15
NDMI	IntDry	Humid	0.28	0.51	0.53	0.40	0.09	0.88	0.76	0.57	1.00	0.06	0.46	0.10
NDVI	Max	Humid	0.07	**< 0.05**	0.12	**< 0.05**	0.27	0.08	0.62	0.45	0.23	0.27	0.63	**< 0.05**
NDVI	Min	Humid	0.42	0.29	0.08	**< 0.05**	0.47	0.10	0.51	0.63	0.64	0.75	0.57	0.06
NDVI	IntDry	Humid	0.31	0.99	0.40	**< 0.05**	0.80	0.60	0.79	0.32	0.73	0.06	0.66	**< 0.05**

Appendix F: P-values of Multiple linear regression between time frames on the percent mortality saplings, small trees, and large trees, conducted on **all forests** on only plots from the **Main Island** of Puerto Rico. Bold indicates a significant p-value of less than 0.05.

Index	Band	Habitat Type	% Sap Mort (2010-2014)	% ST Mort (2010-2014)	% LT Mort (2010-2014)	% Sap Mort (2016-2017)	% ST Mort (2016-2017)	% LT Mort (2016-2017)	% Sap Mort (2017-2018)	% ST Mort (2017-2018)	% LT Mort (2017-2018)	% Sap Mort (2018-2019)	% ST Mort (2018-2019)	% LT Mort (2018-2019)
EVI	Max	Both	0.10	0.54	0.91	0.30	0.38	0.88	0.98	0.27	0.40			
EVI	Min	Both	0.04	0.97	0.18	0.72	0.38	0.81	0.56	0.52	0.40			
EVI	IntDry	Both	0.08	0.61	0.68	0.26	0.71	0.80	0.79	0.86	0.11			
NDMI	Max	Both	0.51	0.32	0.27	0.85	0.10	0.98	0.27	0.16	0.38			
NDMI	Min	Both	0.17	0.76	0.24	0.45	0.07	0.92	0.86	0.28	0.27			
NDMI	IntDry	Both	0.24	0.63	0.98	0.77	0.10	0.79	0.81	0.17	0.08			
NDVI	Max	Both	0.38	0.26	0.09	0.01	0.23	0.08	0.39	0.84	0.56			
NDVI	Min	Both	0.81	0.55	0.15	0.005	0.58	0.11	0.51	0.76	0.54			
NDVI	IntDry	Both	0.72	0.96	0.50	0.03	0.79	0.75	0.71	0.76	0.13			

Appendix G : P-values of Multiple linear regression between time frames on the percent mortality saplings, small trees, and large trees, conducted on **dry forests and humid forests** on only plots from the **Main Island** of Puerto Rico.

			2010-2014	2010-2014	2010-2014	2016-2017	2016-2017	2016-2017	2017-2018	2017-2018	2017-2018	2018-2019	2018-2019	2018-2019
Index	Band	Habitat Type	% Sap Mort	% ST Mort	% LT Mort	% Sap Mort	% ST Mort	% LT Mort	% Sap Mort	% ST Mort	% LT Mort	% Sap Mort	% ST Mort	% LT Mort
EVI	Max	Dry	0.43	0.91	NA	0.12	0.09	NA	0.75	0.85	0.87			
EVI	Min	Dry	0.27	0.97	NA	0.08	0.20	NA	0.91	0.99	0.98			
EVI	IntDry	Dry	0.75	0.74	NA	0.31	0.37	NA	0.49	0.73	0.73			
NDMI	Max	Dry	0.74	0.64	NA	0.44	0.82	NA	0.94	NA	NA			
NDMI	Min	Dry	0.62	0.32	NA	0.33	0.69	NA	0.55	NA	NA			
NDMI	IntDry	Dry	0.87	0.11	NA	0.20	0.57	NA	0.46	NA	NA			
NDVI	Max	Dry	0.75	0.68	NA	0.15	0.98	NA	0.89	0.63	0.60			
NDVI	Min	Dry	0.91	0.16	NA	0.21	0.82	NA	0.85	0.65	0.64			
NDVI	IntDry	Dry	0.63	< **0.05**	NA	0.26	0.36	NA	0.50	0.46	0.42			
EVI	Max	Humid	0.40	0.28	0.96	0.26	0.75	0.71	0.50	0.36	0.22			
EVI	Min	Humid	0.14	0.87	0.19	0.48	0.89	0.86	0.34	0.62	0.18			
EVI	IntDry	Humid	0.33	0.88	0.77	0.35	0.88	0.52	0.67	0.86	0.35			
NDMI	Max	Humid	0.89	< **0.05**	0.30	0.82	< **0.05**	0.85	0.34	0.02	0.53			
NDMI	Min	Humid	0.43	0.98	0.19	0.53	< **0.05**	0.32	0.71	0.47	0.81			
NDMI	IntDry	Humid	0.94	0.92	0.72	0.40	0.09	0.88	0.76	0.57	1.00			
NDVI	Max	Humid	0.13	< **0.05**	0.07	< **0.05**	0.27	0.07	0.62	0.45	0.23			
NDVI	Min	Humid	0.55	0.47	0.16	< **0.05**	0.47	0.10	0.51	0.63	0.64			
NDVI	IntDry	Humid	0.61	0.80	0.82	< **0.05**	0.80	0.60	0.79	0.32	0.73			